Technical University of Munich
TUM School of Engineering and Design
Chair of Timber Structures and Building Construction

Final Report:

Research on Tanzanian Pine for the Use in Construction

Client:

CPS Zanzibar Ltd.
Fumba Town, Zanzibar,
Urban West, Tanzania

represented by: Sebastian Dietzold

Contractor:

Technical University of Munich
School of Engineering and Design
Chair of Timber Structures and Building Construction
Univ.-Prof. Dr.-Ing. Stefan Winter
Arcistr. 21
80333 Munich, Germany

responsible person: Lucas Viereck, M.Sc.

Partner:

Technical University of Munich
School of Engineering and Design
Associate Professorship of Wood Technology
Wood Research Munich
Prof. dr. ir. Jan-Willem van de Kuilen
Winzererstr. 45
80797 Munich, Germany

responsible person: Dr.-Ing. Andriy Kovryga

Date:

18.09.2024

Forword

The tests with the specimens from Tanzania were conducted between September 2023 and May 2024. The successful realization would not have been possible without the help of some important people.

Master student Simon Kramer was of great help, doing the visual grading with student assistants at the Wood Research Munich and executing the mechanical tests with the technicians from the Wood Research Munich and the Materials Testing Institute. He also carried out an extensive evaluation of the results.

Bachelor student Nicole Ebert helped with the fire and gluing tests, independently preparing the specimens and evaluating the results.

Master student Frederic Hanen supported the assessment of the swelling and shrinkage.

Richard Steindl from HBS Berga GmbH & Co. KG and Daniel Stietz from Ante Leimholz GmbH & Co. KG supported the project with technical know-how and by organizing the storage, planing, finger-jointing, and preparation of the specimens.

Martin Bacher from Microtec Srl contributed with his knowledge and made it possible to carry out a machine grading of the specimens.

Frank Hunger from the Materials Testing Institute helped by answering many questions about the testing and grading of the wood.

Many more people were involved in discussions around the project and helped to realize it.

A great thanks to all of them.

Lucas Viereck, Andriy Kovryga

Munich, 29.08.2024

Contents

List of Abbreviations

CLT	cross-laminated timber
DAB	DIN Astansammlung Brett (knot cluster parameter for boards)
DEB	DIN Einzelast Brett (single knot parameter for boards)
DEK	DIN Einzelast Kantholz (single knot parameter for beams)
DSB	DIN Schmalseitenast Brett (narrow side knot parameter for boards)
$E_{dyn,ave,12}$	dynamic modulus of elasticity with average density, normalized to 12 % moisture content in [N/mm²]
$E_{dyn,ind,12}$	dynamic modulus of elasticity with individual density, normalized to 12 % moisture content in [N/mm²]
$E_{m,0}$	bending modulus of elasticity, normalized to 12 % moisture content in [N/mm²]
$E_{m,0,mean}$	mean bending modulus of elasticity in [N/mm²]
$E_{t,0}$	tensile modulus of elasticity, normalized to 12 % moisture content in [N/mm²]
$E_{t,0,mean}$	mean tensile modulus of elasticity in [N/mm²]
EWP	engineered wood product
f_m	bending strength, normalized to a height of 150 mm in [N/mm²]
$f_{m,j}$	bending strength of finger joints, normalized to a height of 150 mm in [N/mm²]
$f_{m,j,k}$	characteristic bending strength of finger joints in [N/mm²]
$f_{m,k}$	characteristic bending strength in [N/mm²]
$f_{t,0}$	tensile strength, normalized to a height of 150 mm in [N/mm²]
$f_{t,0,k}$	characteristic tensile strength in [N/mm²]
MOE	modulus of elasticity
MUF	melamine urea formaldehyde
PRF	phenol resorcinol formaldehyde
PU	polyurethane
rej.	rejected
RH	relative humidity in [%]
STC	standard temperature-time curve
α	differential swelling in % per % change of the moisture content
ρ	density, normalized to 12 % moisture content in [kg/m³]
$\rho_{dyn,12}$	density for the dynamic measurement, normalized to 12 % moisture content in [N/mm²]
ρ_k	characteristic density in [kg/m³]
ρ_{mean}	mean density in [kg/m³]

1 Introduction

1.1 Background

Currently, most constructions in Tanzania are still realized using conventional building materials like steel and concrete. This development, combined with an increasing population, raises the demand for sustainable materials to omit undesired impacts on the environment and global climate. Therefore, the local stakeholders in Tanzania desire to use wood as a building material. Wood species such as pine and eucalyptus are available in Tanzania and show potential for structural application. These two wood species grow in plantations without harming the natural forest stands. Nevertheless, despite extensive use, knowledge about the properties of the local wood needed for the design of timber constructions is missing.

1.2 Objective

To make the application of local timber in Tanzania possible, the material properties (mechanical and physical) of the wood species need to be determined. This project covers preliminary tests on the way to a more extensive testing program. The primary objective is to assess the potential of the Tanzanian local wood resources for structural applications following the framework of European standards.

The project covers the assessment of the mechanical properties (strength and stiffness) of the Tanzania pine in terms of tension and bending. Within the project, the performance of the different grading methods – visual and machine grading – is also assessed and related to the European strength class profiles of EN 338. As the visual grading standard DIN 4074-1 is fitted to Central European softwood species, the adjustment of grading rules to the Tanzanian pine are also included in the scope of the study.

Generally, finger jointing individual timber boards is one of the possibilities for enhancing the quality of timber. Cutting away the local defects, such as large knots, knot clusters, or local inhomogeneities, may upgrade the specimens and lead to higher strength. Therefore, bending tests on finger joints are also part of the study.

The more advanced target for the Tanzanian timber industry is producing engineered wood products (EWP) like glulam and cross-laminated timber (CLT) from the local wood species. This requires a high bond durability of the glued lamellas in the layup. For this purpose, the bonding durability of the Tanzanian pine lamella bonded using a common glue for EWP is tested in delamination test.

In addition, the fire performance (charring rate) of the Tanzanian wood and swelling and shrinkage are measured.

2 Material

The timber specimens of Tanzanian-grown pine (*Pinus patula)* originate from the Sao Hill Plantation in the Tanzanian Highlands (Figure 1). The pine trees at the Sao Hill Plantation have rotation ages between 10 and 18 years (Green Resources 2023). Due to the rapid growth of the trees, the wood is characterized by wide growth rings compared to the ones in Central Europe (cf. Figure 2).

Figure 1: Location of the Sao Hill Plantation in Tanzania (Google Maps)

Figure 2: Timber cross-sections of pinus patula with characteristic wide growth rings

After the primary processing and shipment to Germany, the specimens were stored at Ante Leimholz GmbH & Co. KG, cf. Figure 3. During the storage the rough-sawn wood had dimensions of ca. b/h = 50/100 mm with a length between 4 and 6 m and an average moisture content of 12.5 %.

Figure 3: Timber specimens during the storage at Ante (Ante)

Before being stored inside, the specimens were exposed to changing weather and rain conditions and showed discoloration, mold on the surface, and deformations. For further processing, the specimens were planed to 45/90 mm at Ante and cut to 4 m length. 100 lamellae were randomly chosen for the tensile tests, another 100 lamellae for the bending tests, and another 100 lamellae were finger-jointed. The finger-jointed specimens consisted of two halves from two different lamellae. A one-component polyurethane (PU), Loctite HB S109 (Henkel & Cie. AG) was used to glue the finger joints.

After processing at Ante, the timber was transported to Microtec in Brixen (Italy) for machine grading and afterward to the Technical University of Munich (Germany). While transporting the specimens to Brixen, the specimens were exposed to a high moisture environment for unknown reasons, leading to a moisture content after plaining above the fiber saturation point. This moisture content increase followed by dry conditions at Microtec and TUM has led to significant deformations, see Figure 4.

Figure 4: Deformations of the specimen (warping) due to changes in moisture content before storage at standard climate (left) and after storage in standard climate (right) (Simon Kramer)

3 Methods

3.1 Overview

Table 1 provides a complete overview of the tests that were conducted.

Table 1: Overview of the carried-out tests, corresponding standards, and sample size

Test	Code	No. of specimens
visual grading	DIN 4074-1	200
machine grading	EN 14081-2	200
tensile tests	EN 408	100
bending tests	EN 408	100
bending tests on finger joints	EN 408	100
gluing tests (delamination)	EN 302-2	4
fire tests (charring rate)	prEN 1995-1-2	2
assessment of swelling and shrinkage	DIN 52184	8

The 200 lamellae without finger joints were divided into two equivalent groups for the tensile and bending tests based on the dynamic modulus of elasticity (MOE). All 200 lamellae were ranked on the dynamic MOE and split into two sub-samples for the bending and the tensile tests. The odd numbers were taken for the tensile tests, and the even numbers for the bending tests.

Most of the results of the grading and the mechanical tests are based on the master thesis of Kramer (2024). The results of the gluing tests and fire tests are based on the bachelor thesis of Ebert (2024). The assessment of the swelling and shrinkage is based on the seminar thesis of Hanen (2024).

3.2 Visual Grading

The visual grading was done in the laboratory of the Wood Research Munich according to the German grading standard DIN 4074-1 and involved the following grading characteristics:

- knots
- fiber deviation
- presence of pith
- growth ring width
- checks
- warping
- discolorations
- compression wood
- insect damage

For the 200 specimens, all knots above 5 mm were assessed within the respective test length (cf. section 3.4 and 3.5) based on their size and location. The program developed at the Wood Research Munich was used to acquire the knot data such as knot diameter, location, and size. Different knottiness parameters were evaluated, which relate the knot diameters to the timber's dimensions (height and width). This program allows the grading of boards according to different grading standards, e.g. the German standard for softwood DIN 4074-1.

For the specimens tested in tension, the grading rules for boards of DIN 4074-1 were applied. Those include three different knottiness parameters: single knots (DEB – DIN Einzelast Brett), knot clusters (DAB – DIN Astansammlung Brett), and narrow side knots (DSB – DIN Schmalseitenast Brett). For the specimens tested in edgewise bending, the rules for beams were applied, which include only one knottiness parameter: single knots (DEK – DIN Einzelast Kantholz).

The warping of timber was measured but not considered for the grading, as the material performance was more in focus rather than the further application difficulties. By cutting the timber to the length of test specimens, the warping could be limited for the purpose of the tests. If the grading limits of DIN 4074-1 were applied, the entire batch of timber would have been rejected due to the difficulties mentioned earlier.

The global fiber deviation for all specimens was below DIN 4074-1 specifications. Checks and insect damage were not detected in the present sample. Discolorations were detected on two specimens but were harmless and therefore not considered in the further evaluation. The growth ring width was not considered for the grading initially, as the German grading thresholds do not fit the wood from plantations.

Each specimen could be assigned to a grading class (S7, S10, or S13) or rejected based on these characteristics. The characteristics that determined the grading class assignment were the knottiness parameters DEB, DAB, and DSB or DEK, the presence of pith, and the compression wood. For each grading class, the characteristic values of the strength, MOE, and density were calculated. If these values would fulfill the specifications for a strength class, then it would be possible to assign this strength class to any lamella that fulfills the grading thresholds of the respective grading class and assume the defined values for the mechanical properties like strength and MOE without further mechanical tests.

3.3 Machine Grading

Machine grading has been applied to Tanzanian wood to check the potential of the more advanced technologies. This type of grading makes it possible to assign timber pieces to higher strength classes compared to visual grading and/or to increase the yield. Further advantages are the accuracy, repeatability, and the higher grading speed. On the other hand, grading machines are much more expensive – for visual grading, no special equipment is needed. Machines that only measure the dynamic MOE in combination with visual grading can be a rational compromise.

The machine grading was done in collaboration with Microtec Srl for the 200 specimens for the tensile and bending tests. During the grading procedure, in addition to the machine parameters, the dimensions were assessed using an electrical caliper, the moisture content was measured using the electric resistance method, and the weight was recorded.

The actual machine grading involved several different technologies. First and foremost, the dynamic MOE was measured using the eigenfrequency method. The parameter is known for its high prediction accuracy of the static MOE and the high correlation to the bending and tensile strength for various wood species. Hereby, a longitudinal stress wave in a piece of timber is generated using a hammer, and the vibration is captured contact-free using a laser interferometer. The signal is processed, and the eigenfrequency is calculated by applying a Fourier transform. The dynamic MOE is calculated using eq. (1) by combining the eigenfrequency with the density and the specimens' length.

$$E_{dyn} = 4 \cdot l^2 \cdot f^2 \cdot \rho \quad (1)$$

with: l = length of the specimen in [m]
f = eigenfrequency in [Hz]
ρ = density in [kg/m³]

In addition to the dynamic MOE, a knot detection using an X-ray attenuation method was applied, whereby the density differences between the knots and clear wood were used to detect those structural defects. Moreover, a novel method based on laser scattering has been applied to detect local fiber deviations.

Due to the moisture content issue (cf. section 2), the specimens were regraded in the laboratory of Wood Research Munich regarding the dynamic MOE, moisture content and density. The dynamic MOE was calculated in two different ways, using the individual density of each specimen or a pre-defined species-specific average density. Using the individual density usually gives more accurate results, whereas using the pre-defined average density is more efficient for practical application because the density does not need to be measured.

The machine grading characteristics that were evaluated in this work are the MOE with individual density, MOE with average density, and the density itself.

3.4 Tensile Tests

The tensile tests were executed according to EN 408 with a free test length of 9 x h. The dimensions of the specimens and the test setup are depicted in Figure 5 and Figure 6. The test length was selected in a way that it included the largest weak point, usually a knot or knot cluster.

The tensile MOE was measured within the gauge length of 5 x h with the strain captured using an inductive displacement transducer. The tests were executed displacement-controlled with a constant displacement speed.

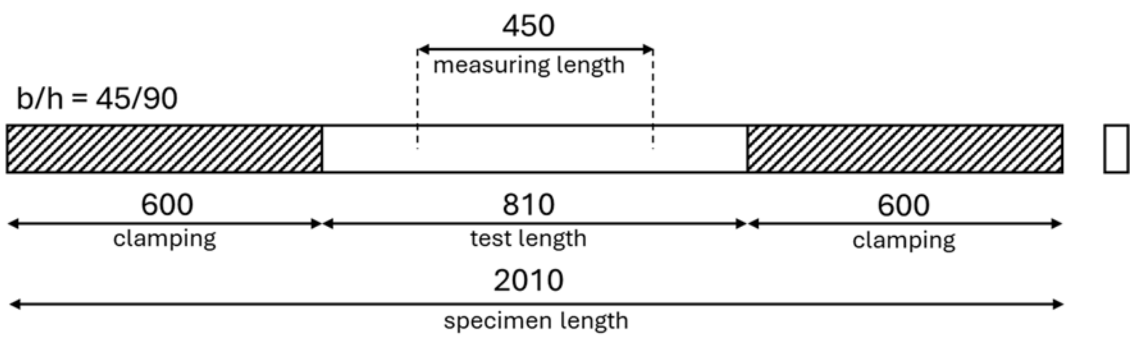

Figure 5: Test setup and dimensions of the tensile test specimens in [mm]

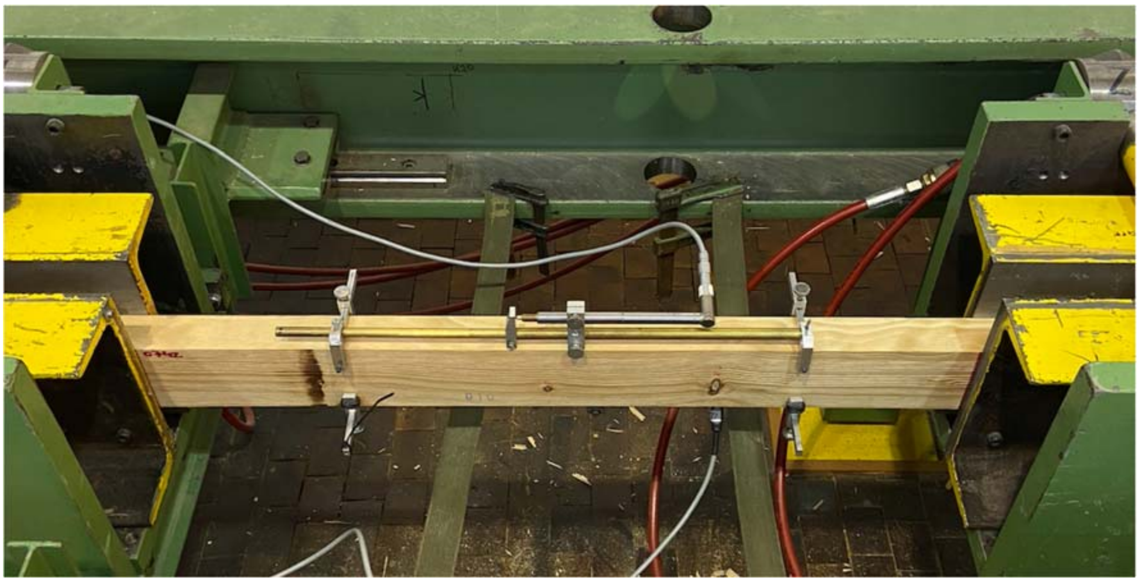

Figure 6: Test setup for the tensile tests in the laboratory (Simon Kramer)

10 specimens were sorted out before the test because of the high level of warping/deformations. The specimens would have been stressed perpendicular to the grain by the clamping. Thus, 90 specimens remained that were tested and evaluated. Before the test, the exact dimensions and the weight of each specimen were determined.

3.5 Bending Tests

The edgewise bending tests on timber pieces were also executed according to EN 408. The dimensions of the specimens and the test setup are depicted in Figure 7 and Figure 8. The location of the test length within the total length of 4 m of the lamellae was again set by selecting the length with the largest weak point. Which side of the specimens was down and thus exposed to tensile stresses was chosen randomly.

The global deflection between the supports, along the whole span, was measured using cable displacement sensors, and the local deflection along the local measuring length was measured using inductive displacement transducers. Thus, a global bending MOE and a local bending MOE were calculated. The tests were executed displacement-controlled with a constant displacement speed.

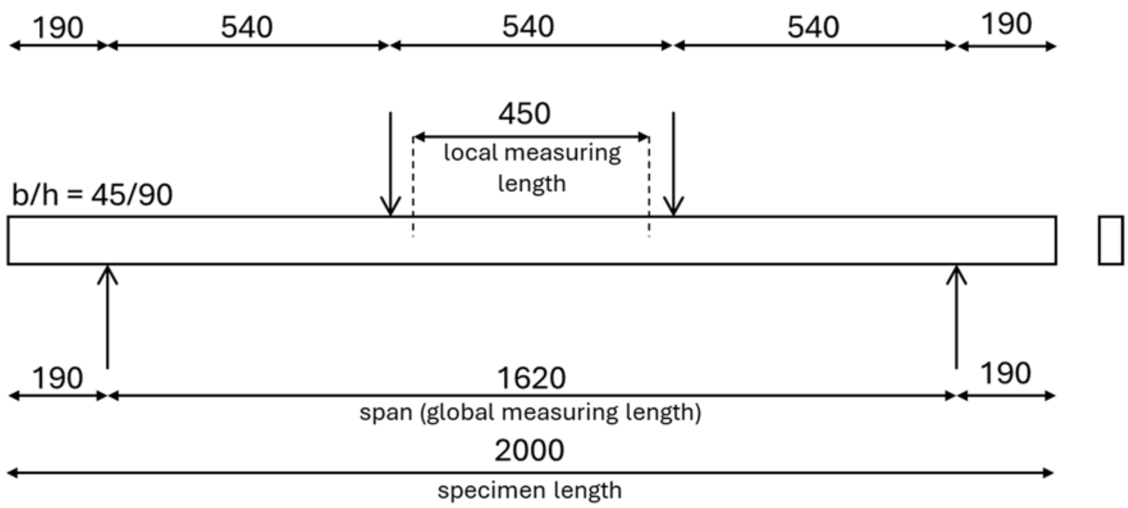

Figure 7: Test setup and dimensions of the bending test specimens in [mm]

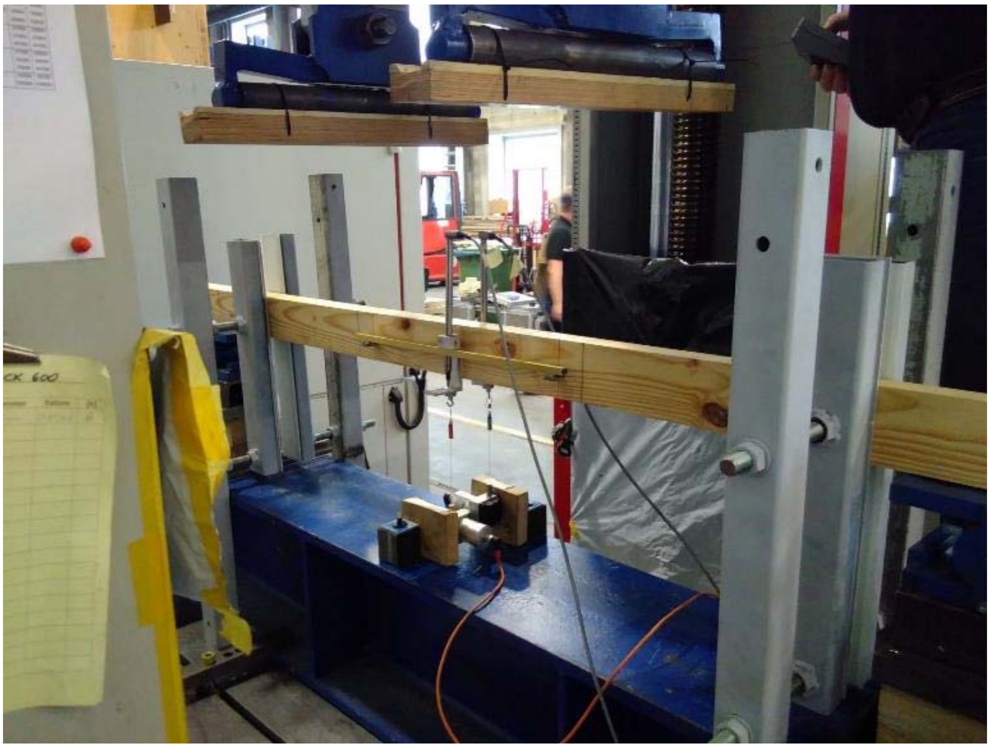

Figure 8: Test setup for the bending tests in the laboratory (Lucas Viereck)

4 specimens had to be sorted out because of rot or previous damage. 1 specimen had to be sorted out because of faulty measurements. Thus, 95 specimens remained that were tested and evaluated. Before the test, the exact dimensions were determined, but the weight of the specimens was not measured.

3.6 Bending Tests on Finger Joints

The flatwise bending tests on finger-jointed specimens were also executed according to EN 408. The test arrangement and the dimensions of the specimens are depicted in Figure 9 and Figure 10.

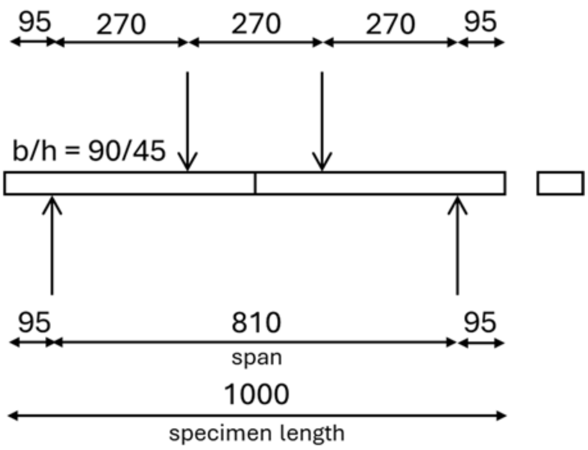

Figure 9: Test setup and dimensions of the bending test specimens with finger joints in [mm]

Figure 10: Test setup for the bending tests on finger joints in the laboratory (Simon Kramer)

For those tests, no displacement was measured because the only purpose was to determine the strength of the finger joints. The tests were executed displacement-controlled with a constant displacement speed. Before the test, the joint's exact dimensions were measured, but the specimens' weight was not determined.

No specimens had to be sorted out so that 100 tests could be carried out.

3.7 Density and Moisture Content

After every test, a 20 mm long clear wood piece was cut out of every specimen according to EN 408; for the specimens with finger joints, two pieces were cut out, one on each side of the joint. Moisture content was measured in accordance with EN 13183-1:2002 by an oven-dry method. The density of the clear wood specimen was calculated by weighting the specimen and determining the volume using the water immersion method by measuring the buoyance force.

All results from the tensile and bending tests were adjusted to the reference moisture content of 12 % according to EN 384.

3.8 Gluing Tests

To produce engineered wood products like glulam or CLT, individual lamellae need to be glued together on their flat edges. Over their life span, the products are exposed to a changing moisture content, which can lead to delamination of the glue lines. According to EN 302-2, delamination tests were carried out to analyze the integrity of the glue line. For the tests, two different types of glue were used: a polyurethane (PU) glue, Jowapur 681.60, and a melamine urea formaldehyde (MUF) glue, Kauramin Glue 690 Liquid with Kauramin Hardener 1690.

To prepare the specimens, 12 pieces of roughly 1000 mm length were cut out of the lamellae. The dimensions and the weight were measured to calculate the density of each piece. Then, the pieces were cut to 500 mm length and planed to 30 mm thickness. Two samples were prepared, each consisting of 6 pieces, cf. Figure 11.

Figure 11: Samples for the preparation of the delamination specimens (Nicole Ebert)

The 6 pieces from each sample were then glued together to form a small glulam beam with the dimensions b/h/l = 90/180/500 mm, cf. Figure 12. For more details on the gluing process, see Appendix A.

Figure 12: Gluing of the delamination specimens (Nicole Ebert)

After the hardening of the glue, the beams were cut to a width of 84 mm. Two specimens were cut from each beam with a length of 75 mm. The finished specimens with the dimensions of b/h/l = 84/180/75 mm are depicted in Figure 13.

Figure 13: Finished delamination specimens (Nicole Ebert)

Before the actual delamination test, each specimen's dimensions and weight were measured. Then, they were put in a pressure tank filled with water for 2.5 hours. When the wood was completely saturated with water, the specimens were taken out of the pressure tank and dried for 18 to 22 hours until the wood was completely dry. This wetting and drying cycle was carried out three times in total. Directly after the last drying, the length of the delamination was measured and related to the total length of the glue lines.

3.9 Fire Tests

The fire tests aimed to determine the one-dimensional charring rate of the Tanzanian wood. This was done according to prEN 1995-1-2 (2023-09).

To prepare the specimens, 24 pieces of roughly 1000 mm length were cut out of the lamellae. The dimensions and the weight were measured to calculate the density of each piece. Based on their density, the pieces were divided into two samples, one with the highest and one with the lowest densities. The 12 pieces of each sample were glued together to form a specimen with a width of 540 mm using the PU Jowapur 681.60. In the inner pieces of each specimen, thermocouples were integrated to measure the temperature in different depths within the wood during the test. After the gluing, the specimens were cut to a length of 590 mm and planed to a thickness of 87 mm to achieve a plane surface. The final dimensions were b/l/t = 540/590/87 mm, cf. Figure 14. A finished specimen is depicted in Figure 15.

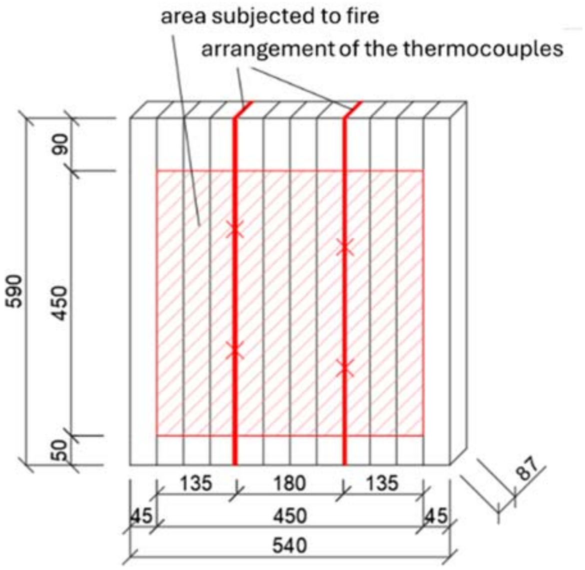

Figure 14: Drawing of the fire test specimens (Nicole Ebert)

Figure 15: Finished fire test specimen with integrated thermocouples (Nicole Ebert)

The specimens were tested in a small fire oven according to DIN 4102-8. The oven had an opening of 450 x 450 mm in one of its walls, which defined the area on the surface of the specimens subjected to the fire. The oven with one of the specimens attached to its side is shown in Figure 16.

Figure 16: Small fire oven with installed test specimen at its side (Lucas Viereck)

The temperature inside the oven was regulated to follow the standard temperature-time curve (STC) according to EN 1363-1, cf. Figure 17. The temperature was increased until the last thermocouple, at a depth of 42 mm, reached a temperature of 300 °C (around this temperature, the wood is considered to start charring).

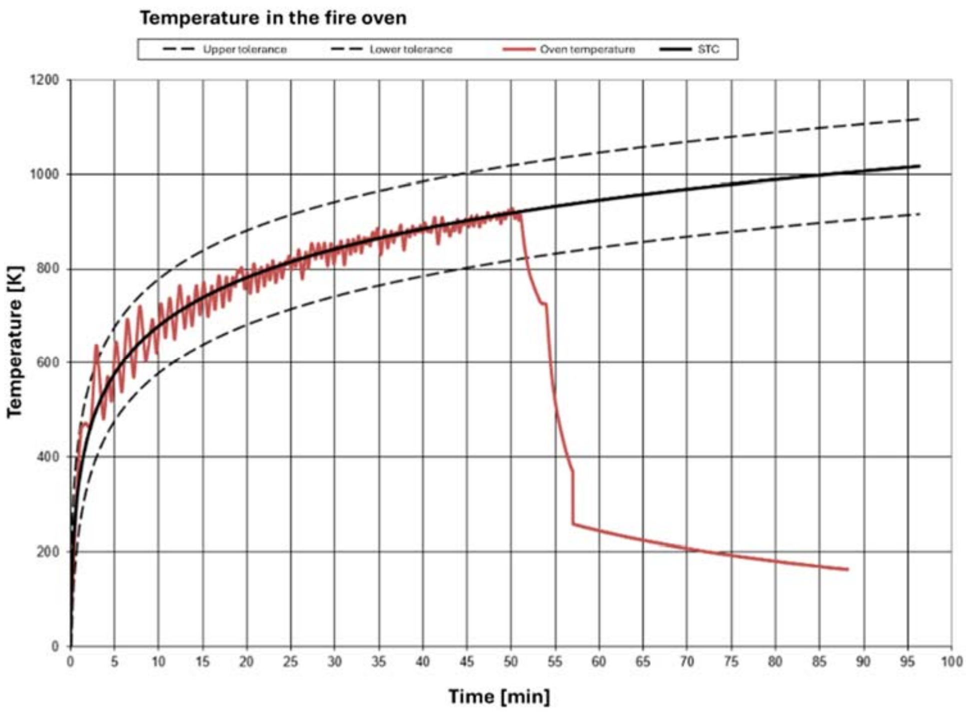

Figure 17: Temperature-time-curve of one of the fire tests

The test was stopped after reaching the target temperature, and the specimen was removed from the oven. Flames were extinguished with water, and after cooling down, the coals were removed from the specimen (cf. Figure 18 and Figure 19). To calculate the charring rate, the measured temperatures of the thermocouples were evaluated over time.

Figure 18: Removal of a fire test specimen from the oven (Nicole Ebert)

Figure 19: Removal of the coals from a fire test specimen (Nicole Ebert)

3.10 Swelling and Shrinkage

Swelling and shrinkage are the changes in the volume of wood due to changes in its moisture content. Usually, it is quantified using the differential swelling and shrinkage coefficients in % change of dimension per % change of moisture content. The coefficients differ in the wood's three anatomical directions radial, tangential, and longitudinal.

Small specimens were cut out of the wood to measure the swelling and shrinkage according to DIN 52184. The specimens for the radial and tangential measurements had dimensions of b/h/l = 20/20/10 mm, and those for the longitudinal measurements had dimensions of b/h/l = 20/20/100 mm. For each case, two specimens with wide growth rings and two with thin growth rings were prepared to assess the influence of the growth ring width on the swelling and shrinkage. The test specimens are shown in Figure 20.

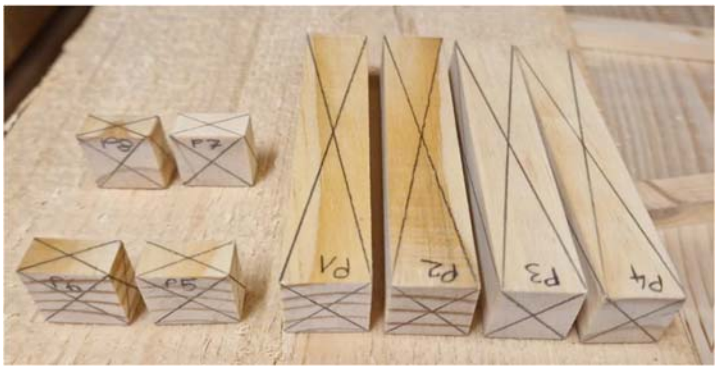

Figure 20: Specimens for the measurement of the swelling and shrinkage – left: specimens for the radial and tangential measurement, right: specimens for the longitudinal measurement (Nicole Ebert)

During the test, the specimens were subjected to different climates and stored in each environment long enough to reach equilibrium humidity. After reaching equilibrium, the specimens' dimensions and weight were measured.

1. standard climate: 20 °C temperature and 65 % relative humidity (RH)
2. moist climate: 20 °C and 85 % RH
3. dry climate: 20 °C and 35 % RH
4. drying at 103 °C
5. emersion in water to reach a fully saturated condition

The swelling and shrinkage coefficients could be calculated from the difference in the dimensions at each climate.

3.11 Evaluation Methods for the Mechanical Tests

The statistical evaluation of the results from the mechanical tests was performed according to EN 384 and EN 14358. For this purpose, the strength values were adjusted to a height of 150 mm, and the MOE and density values were adjusted to 12 % moisture content following the regulations of EN 384. Characteristic mean and 5^{th} percentile values were calculated for the assignment to the strength classes.

Generally, EN 384 requires testing several representative sub-samples (different origins, sawmills, etc.). The so-called k_n factor, a reduction factor depending on the number of sub-samples, is applied to the characteristic value. No reduction is applied for 5 sub-samples; for 1 sub-sample, the factor is 0.88 for the MOE and density, and 0.7 for the characteristic strength. However, this factor was not applied within this study due to its preliminary character. In following investigations, several samples from different origins should be tested to avoid reduction.

An optimum grading according to EN 14081-2 was performed to determine the investigated samples' theoretical maximum potential. This means, the highest number of specimens was determined to fulfill the requirements of a particular strength class.

In any timber processing company, however, the theoretical maximum yields of the optimum grading cannot be reached because the properties that determine the strength class (strength, MOE, and density of each lamella) are unknown. These properties must be estimated using non-destructive methods. Standard non-destructive methods are the visual and machine grading evaluated in this work.

3.12 Strength class requirements

The specifications of the used tensile strength classes are given in Table 2. The specifications of the bending strength classes are given in Table 3.

Table 2: Specifications of the tensile strength classes according to EN 338

strength class	specifications		
	$f_{t,0,k}$ [N/mm²]	$E_{t,0,mean}$ [N/mm²]	ρ_k [kg/m³]
T8	8	7000	290
T9	9	7500	300
T10	10	8000	310
T11	11	9000	320
T12	12	9500	330
T13	13	10000	340
T14	14	11000	350
T15	15	11500	360
T16	16	11500	370
T18	18	12000	380
T21	21	13000	390
T22	22	13000	390
T24	24	13500	400
T26	26	14000	410

Table 3: Specifications of the bending strength classes according to EN 338

strength class	specifications		
	$f_{m,k}$ [N/mm²]	$E_{m,0,mean}$ [N/mm²]	ρ_k [kg/m³]
C14	14	7000	290
C16	16	8000	310
C18	18	9000	320
C20	20	9500	330
C22	22	10000	340
C24	24	11000	350
C27	27	11500	360
C30	30	12000	380
C35	35	13000	390
C40	40	14000	400

4 Results

4.1 Tensile Tests

4.1.1 Overall Results

The statistical results of the whole sample of tensile test specimens are shown in Table 4. The relevant values for the assignment of a strength class are highlighted.

Table 4: Statistical values of the tensile tests according to EN 14358

n = 90	$f_{t,0}$ [N/mm²]	$E_{t,0}$ [N/mm²]	ρ [kg/m³]
mean	13.6	***7204 ****	429
variation coefficient	47.3 %	38.2 %	18.9 %
5th percentile	***4.8***	2343	***288***

** According to EN 384, the mean MOE should be divided by a factor of 0.95 for the determination of the characteristic value.*

Since the characteristic 5th percentile of the tensile strength is below the lowest existing strength class in EN 338 (T8 with $f_{t,0,k}$ = 8 N/mm², cf. Table 2), the ungraded sample cannot be assigned to any strength class.

4.1.2 Optimum Grading

The results of the optimum grading are given in Table 5 and Figure 21. The highest strength class that could be reached is T22.

Table 5: Results of the optimum grading of the tensile test specimens

strength class	characteristic values			yield
	$f_{t,0,k}$ [N/mm²]	$E_{t,0,mean}$ [N/mm²]	ρ_k [kg/m³]	
T8	8.0	8153	311	82 %
T9	9.1	8396	317	72 %
T10	10.1	8842	328	62 %
T11	11.1	9176	331	53 %
T12	12.2	9565	331	43 %
T13	13.8	10084	351	32 %
T14	15.8	13051	430	11 %
T15	15.8	13051	430	11 %
T16	16.6	13311	452	10 %
T18	19.1	13588	437	9 %
T21	22.2	13677	447	8 %
T22	22.2	13677	447	8 %
T24	-	-	-	0 %
T26	-	-	-	0 %

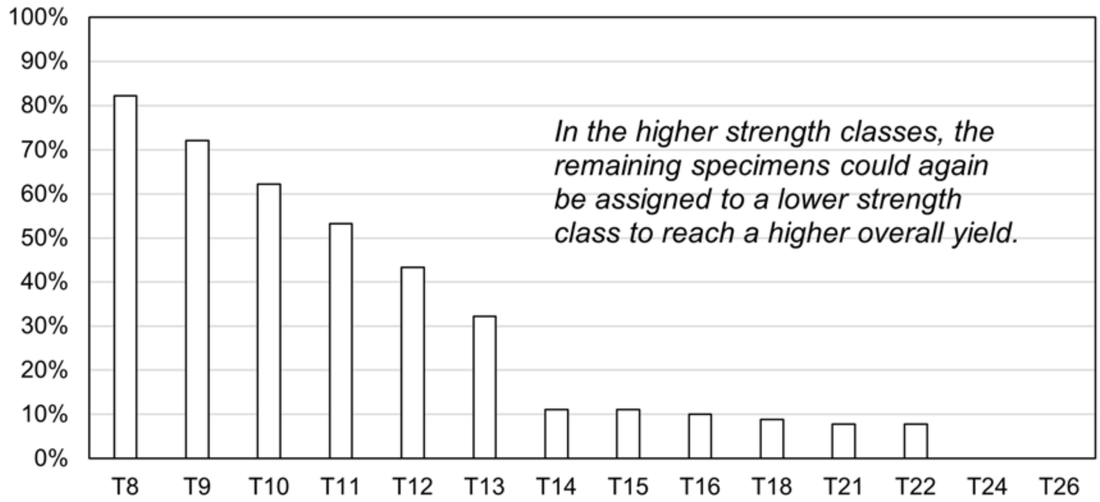

Figure 21: Maximum possible yield per tensile strength class based on the optimum grading

4.1.3 Visual Grading

Visual Grading According to DIN 4074-1

3 specimens were sorted out because of a knot going through the whole cross-section. These would also be sorted out in any processing company before the actual grading. Thus, only 87 specimens remained. The results of the visual grading are presented in Table 6.

Table 6: Characteristic values of the grading classes based on the visual grading according to DIN 4074-1

grading class	characteristic values			yield	assignment to strength class
	$f_{t,0,k}$ [N/mm²]	$E_{t,0,mean}$ [N/mm²]	ρ_k [kg/m³]		
rej.	-	-	-	8 %	-
S7	6.6	7241	300	49 %	-
S10	5.4	8138	271	43 %	-
S13	-	-	-	0 %	-

8 % of all specimens could not be assigned to any grading class and were rejected; 92 % could be assigned to the grading classes S7 or S10. However, none of the grading classes can be assigned to a strength class because the characteristic property values are lower than the specifications (cf. Table 2).

Still, as the optimum grading showed, the assessed sample does have the potential to reach even high strength classes. The specifications for the grading classes in DIN 4074-1 are obviously unsuitable for Tanzanian-grown pine. Therefore, an optimized visual grading with adjusted specifications was performed.

Optimized Visual Grading

First, to determine which grading characteristics would be suitable for an optimized visual grading, the correlations between the different grading characteristics and the measured strength of each specimen were calculated, see Table 7.

Table 7: Correlations between the tensile strength and selected visual grading characteristics of the tensile test specimens

	DEB	DAB	DSB	pith	growth ring width	compression wood
$f_{t,0}$	-0.35	-0.42	-0.08	-0.26	-0.60	0.59

The correlation of the strength with the knottiness parameters DEB and DAB is significantly higher than with the parameter DSB. The pith has a low correlation, whereas the growth ring width has a relatively high correlation. Therefore, the parameters DEB, DAB, and growth ring width were chosen for the optimized visual grading. The compression wood was neglected because it is more difficult to measure.

Analyzing all possible combinations, the following specifications that allow the assignment of strength classes could be identified, see Table 8. The yield of the different strength classes is also presented in Figure 22.

Table 8: Specifications and characteristic values of the possible new grading classes based on the optimized visual grading for the tensile tests

specifications			characteristic values			yield	assignment to strength class
DEB	DAB	growth ring width [mm]	$f_{t,0,k}$ [N/mm²]	$E_{t,0,mean}$ [N/mm²]	ρ_k [kg/m³]		
< 0.6	< 0.7	< 14	8.4	9037	343	67 %	T8
< 0.3	< 0.6	< 10	9.5	9748	351	37 %	T9
< 0.5	< 0.6	< 4	10.8	11321	399	14 %	T10
< 0.3	< 0.6	< 4	12.6	11570	381	9 %	T12

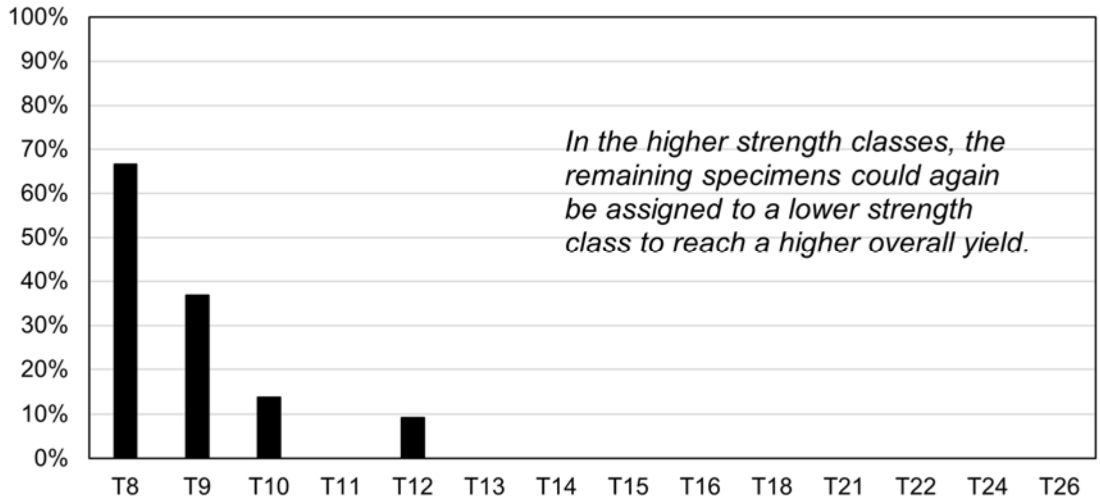

Figure 22: Yield per tensile strength class based on the optimized visual grading

The highest strength class that can be reached is T12, although only with a yield of 9 %. Of course, the same group of specimens that reached T12 can also be assigned to T11. The yield of the lowest strength class, T8, is sufficient. One could also define a lower strength class like T7, which would probably reach a higher yield. However, this was not assessed within this project.

4.1.4 Machine Grading

The same three specimens were sorted out as for visual grading because the knot going through the cross-section did not allow the measurement of the eigenfrequency. Thus, 87 specimens were examined.

The identified specifications for the three independent grading parameters for the assignment of strength classes are shown in Table 9, Table 10, and Table 11. The yields of the different strength classes are also presented in Figure 23. The pre-defined average density was taken as 460 kg/m³.

Table 9: Specifications for the machine grading using the dynamic MOE with individual density and respective characteristic values of the tensile test specimens

grading thresholds	characteristic values			yield	assignment to strength class
$E_{dyn,ind,12}$ [N/mm²]	$f_{t,0,k}$ [N/mm²]	$E_{t,0,mean}$ [N/mm²]	ρ_k [kg/m³]		
> 6727	8.0	8916	342	70 %	T8
> 10672	9.1	11220	427	23 %	T9
> 11270	10.3	12024	414	16 %	T10
> 12297	15.6	12943	440	11 %	T15
> 12511	16.6	13311	452	10 %	T16
> 14004	21.1	14274	444	6 %	T21

Table 10: Specifications for the machine grading using the dynamic MOE with average density and respective characteristic values of the tensile test specimens

grading thresholds	characteristic values			yield	assignment to strength class
$E_{dyn,ave,12}$ [N/mm²]	$f_{t,0,k}$ [N/mm²]	$E_{t,0,mean}$ [N/mm²]	ρ_k [kg/m³]		
> 8126	8.1	9396	336	55 %	T8
> 9328	9.5	10480	359	30 %	T9
> 9989	10.8	11075	357	22 %	T10
> 10178	12.2	11322	352	20 %	T12
> 10816	14.9	12792	386	10 %	T14
> 10894	16.4	13253	402	9 %	T16
> 11230	20.3	14066	407	6 %	T18

Table 11: Specifications for the machine grading using the density and respective characteristic values of the tensile test specimens

grading thresholds	characteristic values			yield	assignment to strength class
$\rho_{dyn,12}$ [kg/m³]	$f_{t,0,k}$ [N/mm²]	$E_{t,0,mean}$ [N/mm²]	ρ_k [kg/m³]		
> 468	8.2	9663	381	47 %	T8

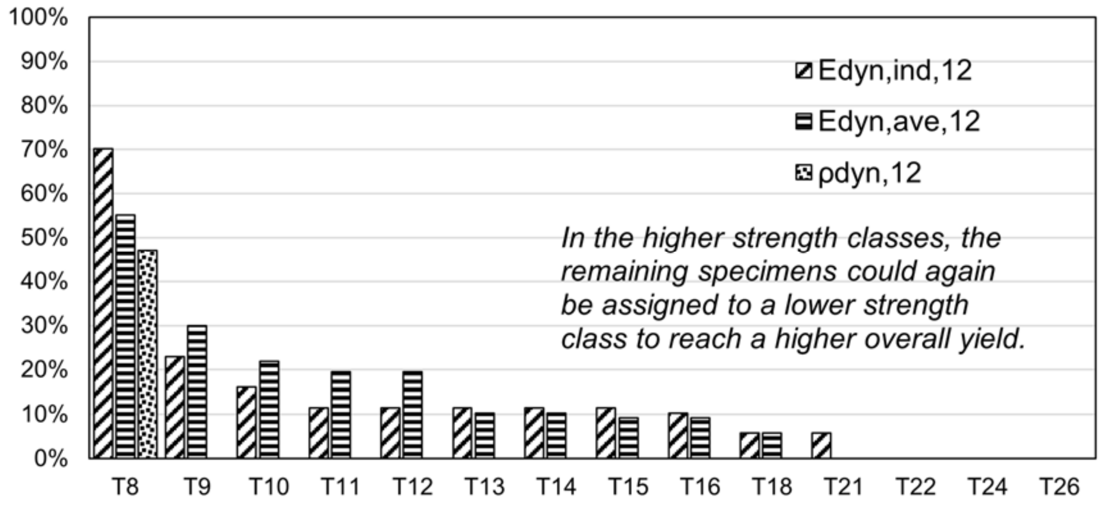

Figure 23: yield per tensile strength class based on the machine grading

With the machine grading using the dynamic MOE calculated with the individual density, the highest strength class can be reached, T21. The dynamic MOE using the average density yields only T18 but is otherwise comparable. The density as a single predictor is the least effective strength grading method because only T8 can be reached.

4.1.5 Combined Visual and Machine Grading

Considering the previous results, the combined grading approach using the visual grading parameters DEB, DAB, and growth ring width and the machine grading parameters dynamic MOE with average density and with individual density was investigated.

Analyzing all possible combinations, the following possible specifications could be identified that allow the assignment of strength classes, see Table 12. The yield of the different strength classes is also presented in Figure 22.

Table 12: Specifications for the combined grading DEB + DAB + growth ring width + dynamic MOE with average density and respective characteristic values of the tensile test specimens

grading thresholds				characteristic values				
DEB	DAB	growth ring width [mm]	$E_{dyn,ave,12}$ [N/mm²]	$f_{t,0,k}$ [N/mm²]	$E_{t,0,mean}$ [N/mm²]	ρ_k [kg/m³]	yield	assignment to strength class
< 0.6	< 0.7	< 14	> 5000	8.4	9037	343	67 %	T8
< 0.3	< 0.6	< 12	> 8000	9.0	9734	350	39 %	T9
< 0.5	< 0.6	< 4	> 7000	10.8	11321	399	14 %	T10
< 0.4	< 0.7	< 12	> 10000	11.9	11296	345	18 %	T11
< 0.5	< 0.7	< 12	> 10000	12.2	11322	352	20 %	T12
< 0.5	< 0.5	< 6	> 10000	13.3	12404	373	11 %	T13
< 0.4	< 0.6	< 6	> 11000	14.4	13715	372	7 %	T14
< 0.5	< 0.6	< 6	> 11000	15.5	13381	383	8 %	T15
< 0.5	< 0.5	< 4	> 10000	16.2	13049	389	7 %	T16

Table 13: Specifications for the combined grading DEB + DAB + dynamic MOE with average density and respective characteristic values of the tensile test specimens

grading thresholds			characteristic values			yield	assignment to strength class
DEB	DAB	$E_{dyn,ave,12}$ [N/mm²]	$f_{t,0,k}$ [N/mm²]	$E_{t,0,mean}$ [N/mm²]	ρ_k [kg/m³]		
< 0.3	< 0.7	> 8000	8.0	9179	323	47 %	T8
< 0.3	< 0.5	> 11000	12.5	13532	308	5 %	T9
< 0.3	< 0.5	> 12000	10.7	14781	318	2 %	T10
< 0.4	< 0.7	> 10000	11.9	11296	345	18 %	T11
< 0.5	< 0.7	> 10000	12.2	11322	352	20 %	T12
< 0.4	< 0.6	> 11000	14.4	13715	372	7 %	T14
< 0.5	< 0.6	> 11000	15.5	13381	383	8 %	T15
< 0.5	< 0.5	> 11000	16.2	13444	376	7 %	T16

Table 14: Specifications for the combined grading DEB + DAB + growth ring width + dynamic MOE with individual density and respective characteristic values of the tensile test specimens

grading thresholds				characteristic values			yield	assignment to strength class
DEB	DAB	growth ring width [mm]	$E_{dyn,ind,12}$ [N/mm²]	$f_{t,0,k}$ [N/mm²]	$E_{t,0,mean}$ [N/mm²]	ρ_k [kg/m³]		
< 0.4	< 0.7	< 16	> 6000	8.1	8902	328	69 %	T8
< 0.3	< 0.6	< 14	> 7000	9.0	9545	351	44 %	T9
< 0.4	< 0.6	< 4	> 8000	10.3	11281	394	13 %	T10
< 0.3	< 0.5	< 4	> 11000	12.6	12902	329	5 %	T11
< 0.3	< 0.6	< 4	> 10000	12.6	11570	381	9 %	T12
< 0.3	< 0.6	< 4	> 13000	13.6	13561	376	5 %	T13
< 0.4	< 0.7	< 6	> 12000	14.9	13095	443	10 %	T14
< 0.3	< 0.6	< 6	> 13000	15.8	13811	395	6 %	T15
< 0.3	< 0.6	< 6	> 12000	17.4	13715	423	7 %	T16
< 0.4	< 0.6	< 6	> 12000	18.5	13912	441	8 %	T18
< 0.3	< 0.5	< 6	> 12000	21.3	13873	434	6 %	T21
< 0.4	< 0.5	< 6	> 12000	22.3	14084	459	7 %	T22

Table 15: Specifications for the combined grading DEB + DAB + dynamic MOE with individual density and respective characteristic values

grading thresholds			characteristic values			yield	assignment to strength class
DEB	DAB	$E_{dyn,ind,12}$ [N/mm²]	$f_{t,0,k}$ [N/mm²]	$E_{t,0,mean}$ [N/mm²]	ρ_k [kg/m³]		
< 0.4	< 0.7	> 7000	8.2	9102	346	63 %	T8
< 0.3	< 0.7	> 8000	9.2	9626	353	43 %	T9
< 0.3	< 0.5	> 15000	10.7	14781	318	2 %	T10
< 0.4	< 0.7	> 12000	14.9	13095	443	10 %	T14
< 0.3	< 0.6	> 13000	15.8	13811	395	6 %	T15
< 0.3	< 0.6	> 12000	17.4	13715	423	7 %	T16
< 0.4	< 0.6	> 12000	18.5	13912	441	8 %	T18
< 0.3	< 0.5	> 12000	21.3	13873	434	6 %	T21
< 0.4	< 0.5	> 12000	22.3	14084	459	7 %	T22

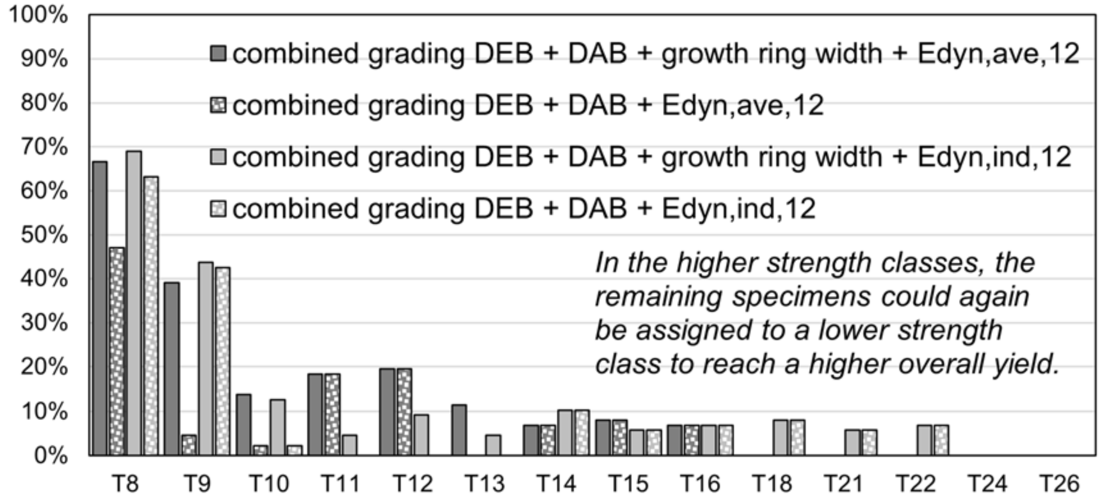

Figure 24: Yield per tensile strength class based on the combined visual and machine grading

4.1.6 Comparison of the Different Grading Methods

To compare the different grading methods, Figure 25 and Figure 26 show the yield per strength class for all grading methods. For some grading methods, grading to lower strength classes let to lower or even 0 yields, while at the same time, grading to a higher class had a higher yield (e.g. T11 and T12 in Figure 22). In those cases, the yield of the higher class (T12) was also assigned to the lower classes (T11), because the same group of specimens would of course also fulfill the specifications for the lower strength class. The reason this occurs is that, for each group of specimens, the highest possible strength class was determined.

Figure 27 shows the highest overall strength class that can be reached by each method.

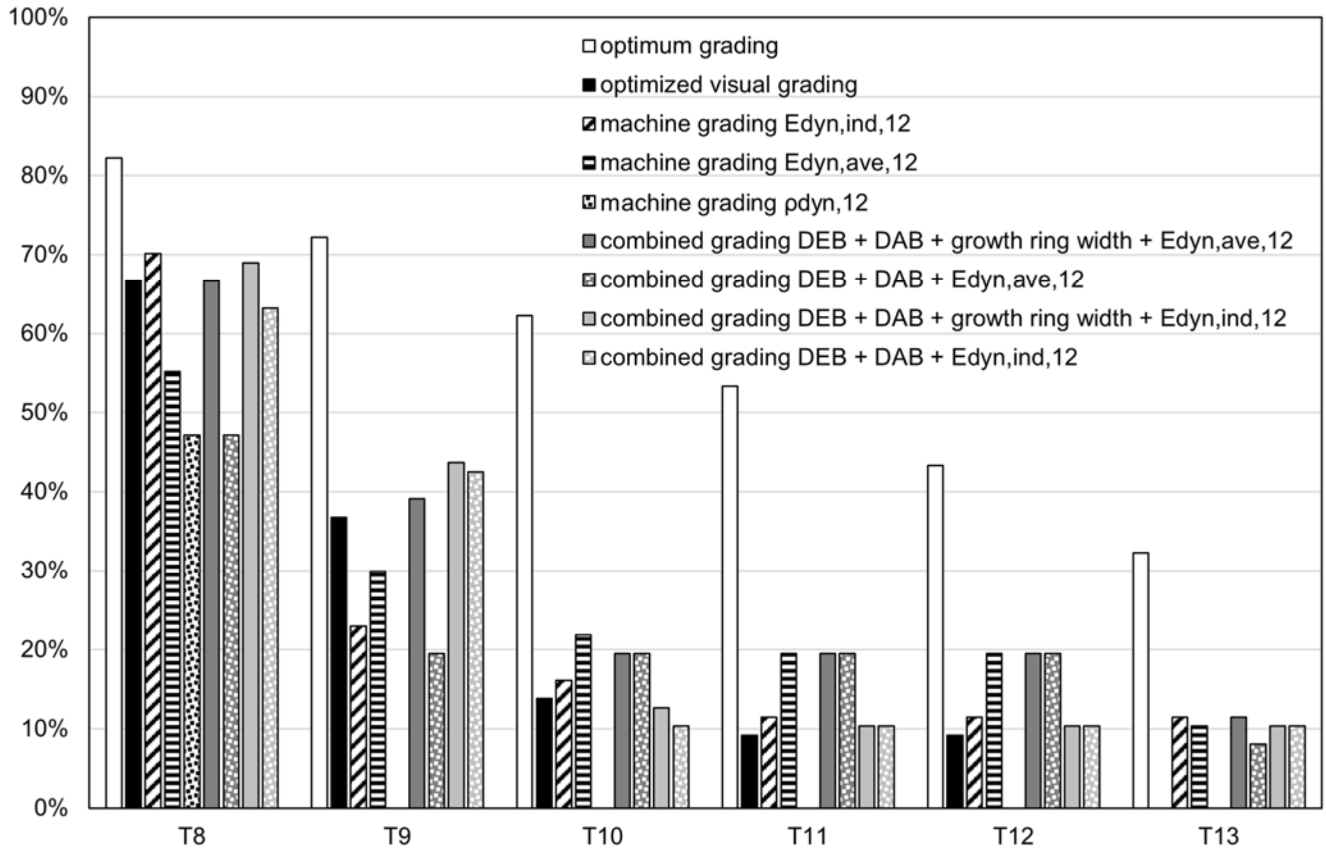

Figure 25: Comparison of the yield of the different grading methods for strength classes T8 to T13

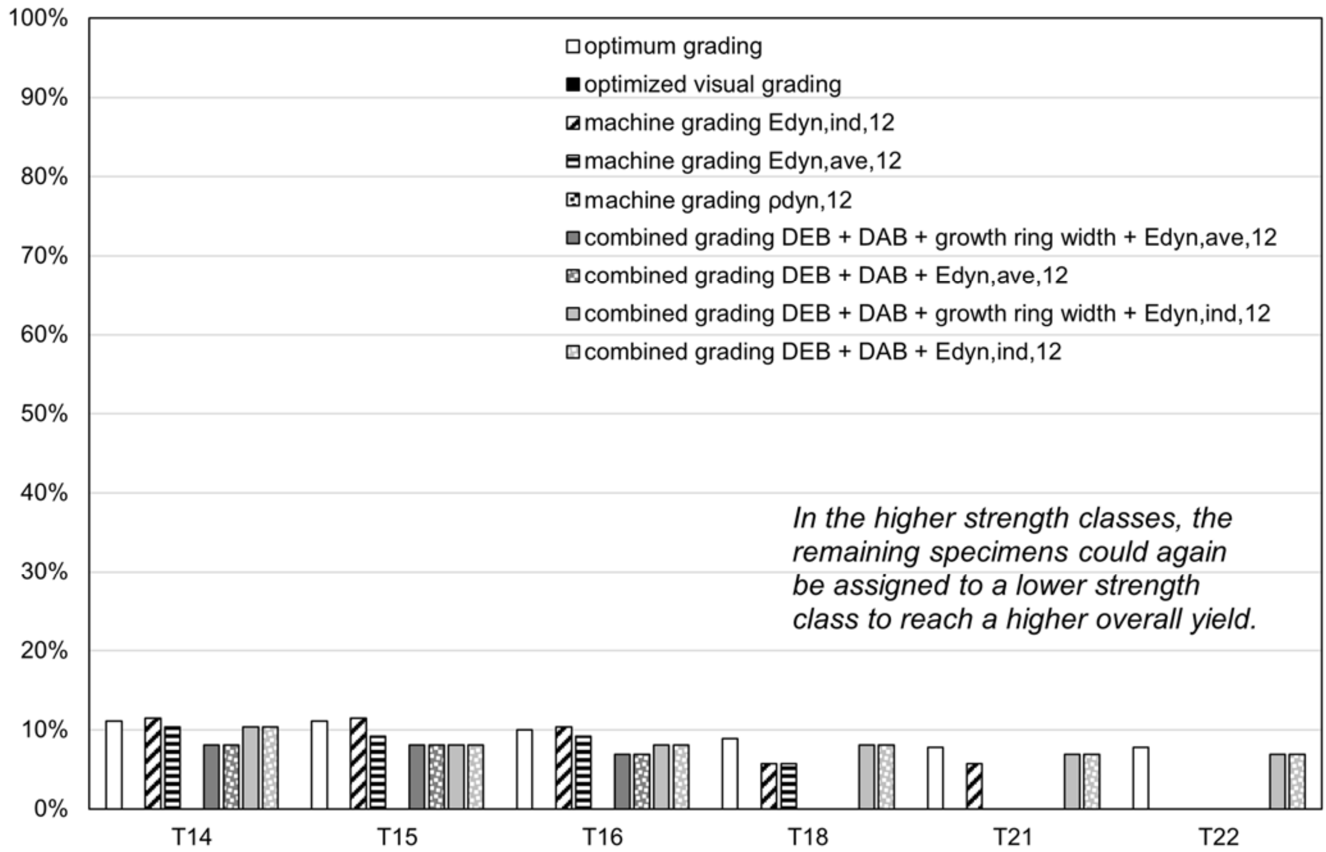

Figure 26: Comparison of the yield of the different grading methods for strength classes T14 to T22

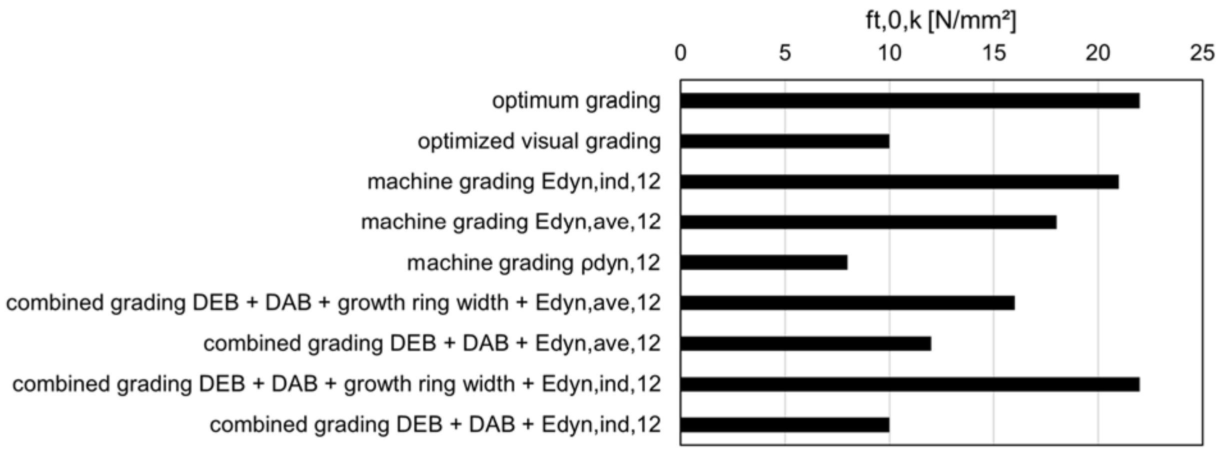

Figure 27: Maximum strength class that the different grading methods can reach

4.2 Bending Tests

4.2.1 Overall Results

The statistical results according to EN 14358 of the whole sample of bending test specimens are shown in Table 16. The relevant values for the assignment of a strength class are highlighted.

Table 16: Statistical values of the bending tests according to EN 14358

n = 95	**f_m [N/mm²]**	**$E_{m,0}$ [N/mm²]**	**ρ [kg/m³]**
mean	24.5	***6694*** *	422
variation coefficient	42.2 %	36.7 %	18.4 %
5^{th} percentile	***9.7***	2361	***287***

** According to EN 384, the mean MOE should be divided by a factor of 0.95 for the determination of the characteristic value.*

Since the characteristic 5^{th} percentile of the tensile strength is below the lowest existing strength class in EN 338 (C14 with $f_{m,k}$ = 14 N/mm², cf. Table 3), the ungraded sample cannot be assigned to any strength class.

4.2.2 Optimum Grading

The results of the optimum grading are given in Table 17 and Figure 28. The highest strength class that could be reached is C27.

Table 17: Results of the optimum grading of the bending test specimens

strength class	characteristic values			yield
	$f_{m,k}$ [N/mm²]	$E_{m,0,mean}$ [N/mm²]	ρ_k [kg/m³]	
C14	14.2	7541	306	87 %
C16	18.2	8022	319	71 %
C18	23.8	9000	337	44 %
C20	26.3	9513	363	29 %
C22	22.8	10941	377	21 %
C24	25.7	11666	382	9 %
C27	27.8	11762	408	8 %
C30	-	-	-	0 %
C35	-	-	-	0 %
C40	-	-	-	0 %

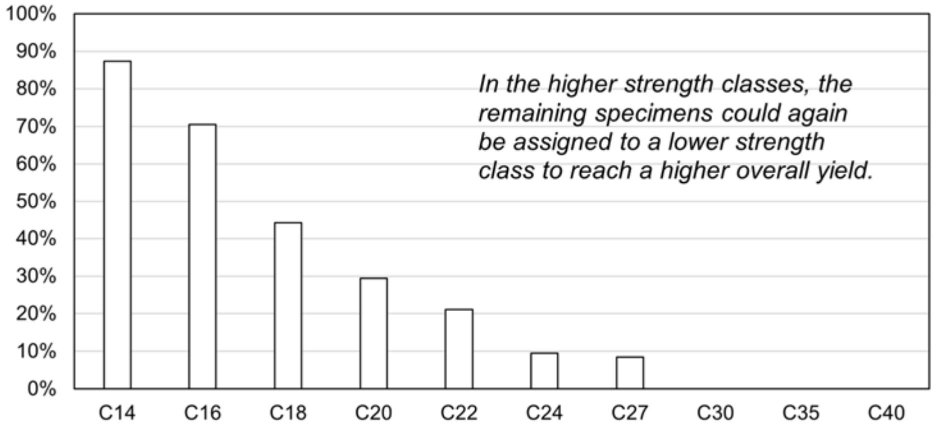

Figure 28: Maximum possible yield per bending strength class based on the optimum grading

4.2.3 Visual Grading

Visual Grading According to DIN 4074-1

The results of the visual grading are presented in Table 18.

Table 18: Characteristic values of the grading classes based on the visual grading according to DIN 4074-1

grading class	characteristic values			yield	assignment to strength class
	$f_{m,k}$ [N/mm²]	$E_{m,0,mean}$ [N/mm²]	ρ_k [kg/m³]		
rej.	-	-	-	19 %	-
S7	7.3	6981	274	49 %	-
S10	12.7	6704	277	31 %	-
S13	-	-	-	1 %	-

19 % of all specimens could not be assigned to any grading class and were rejected; 80% could be assigned to the grading classes S7 or S10. Only 1 specimen (1 %) could be assigned to S13, which was insufficient to determine characteristic values. Again, none of the grading classes can be assigned to a strength class because the characteristic values of the mechanical properties are lower than the

specifications (cf. Table 3). As the results of the optimum grading also show high potential for the bending strength classes, an optimized visual grading with adjusted specifications was performed.

Optimized Visual Grading

To determine which grading characteristics would be suitable for an optimized visual grading, the correlations between the different grading characteristics and the measured strength of each specimen were calculated, see Table 19.

Table 19: Correlations between the bending strength and selected visual grading characteristics of the bending test specimens

	DEK	pith	growth ring width	compression wood
f_m	-0.27	-0.13	-0.43	0.36

The knottiness parameter DEK and the growth ring width have the highest correlation with the strength and were chosen for the optimized visual grading.

Analyzing all possible combinations, the following specifications that allow the assignment of strength classes could be identified, see Table 20. The yield of the different strength classes is also presented in Figure 29.

Table 20: Specifications and characteristic values of the possible new grading classes based on the optimized visual grading for the bending tests

grading thresholds		characteristic values			yield	assignment to strength class
DEK	growth ring width [mm]	$f_{m,k}$ [N/mm²]	$E_{m,0,mean}$ [N/mm²]	ρ_k [kg/m³]		
< 1.0	< 6	14.8	9301	389	33 %	C14
< 0.3	< 6	19.0	8457	320	3 %	C16

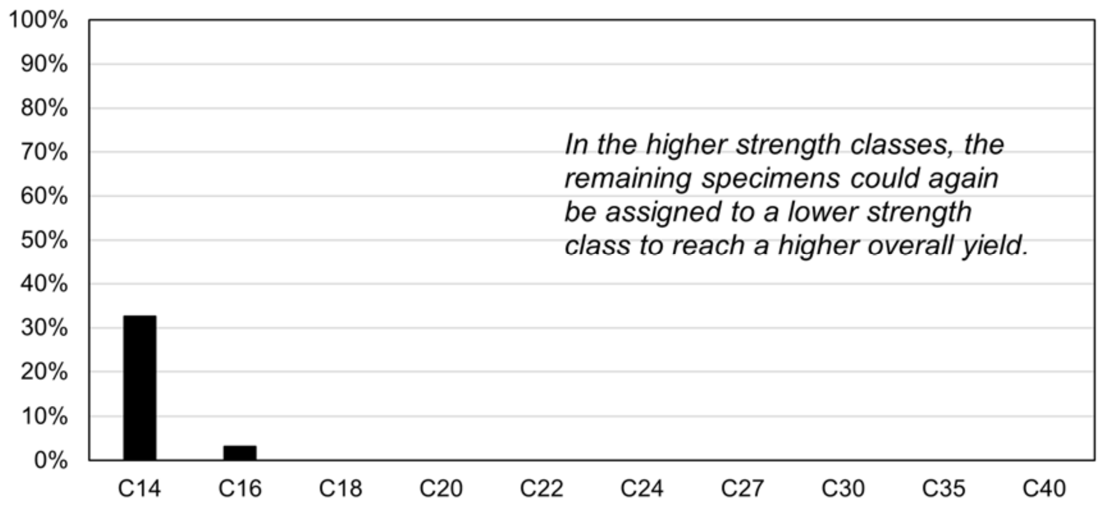

Figure 29: Yield per bending strength class based on the optimized visual grading

The highest strength class that can be reached is C14, although only with a yield of 3 %. Compared to the tensile tests, the yield of the lowest strength class C14 is also relatively low. The definition of a lower-strength class like C12 could lead to better results. However, this was not assessed within this project.

4.2.4 Machine Grading

The identified specifications for the grading using the three different machine grading parameters are shown in Table 21, Table 22, and Table 23. The yields for grading the timber to the various strength classes are also presented in Figure 30.

In contrast to the tensile test specimens, the grading with the density gives the best results; even the strength class C22 can be reached. In the lowest strength class, C14, all three methods are equal.

Table 21: Specifications for the machine grading using the dynamic MOE with individual density and respective characteristic values of the bending test specimens

grading thresholds	characteristic values			yield	assignment to strength class
$E_{dyn,ind,12}$ [N/mm²]	$f_{m,k}$ [N/mm²]	$E_{m,0,mean}$ [N/mm²]	ρ_k [kg/m³]		
> 8392	15.3	9030	370	47 %	C14
> 8720	16.5	9315	376	42 %	C16
> 13827	18.9	9761	491	4 %	C18

Table 22: Specifications for the machine grading using the dynamic MOE with average density and respective characteristic values of the bending test specimens

grading thresholds	characteristic values			yield	assignment to strength class
$E_{dyn,ave,12}$ [N/mm²]	$f_{m,k}$ [N/mm²]	$E_{m,0,mean}$ [N/mm²]	ρ_k [kg/m³]		
> 8274	14.7	8762	348	47 %	C14
> 8364	16.1	8920	358	45 %	C16
> 10011	18.6	9844	373	21 %	C18

Table 23: Specifications for the machine grading using the density and respective characteristic values of the bending test specimens

grading thresholds	characteristic values			yield	assignment to strength class
$\rho_{dyn,12}$ [kg/m³]	$f_{m,k}$ [N/mm²]	$E_{m,0,mean}$ [N/mm²]	ρ_k [kg/m³]		
> 476	14.2	8758	388	49 %	C14
> 503	17.7	9313	408	27 %	C16
> 523	18.5	9368	412	17 %	C18
> 546	21.5	10466	452	11 %	C20
> 560	22.4	10340	453	9 %	C22

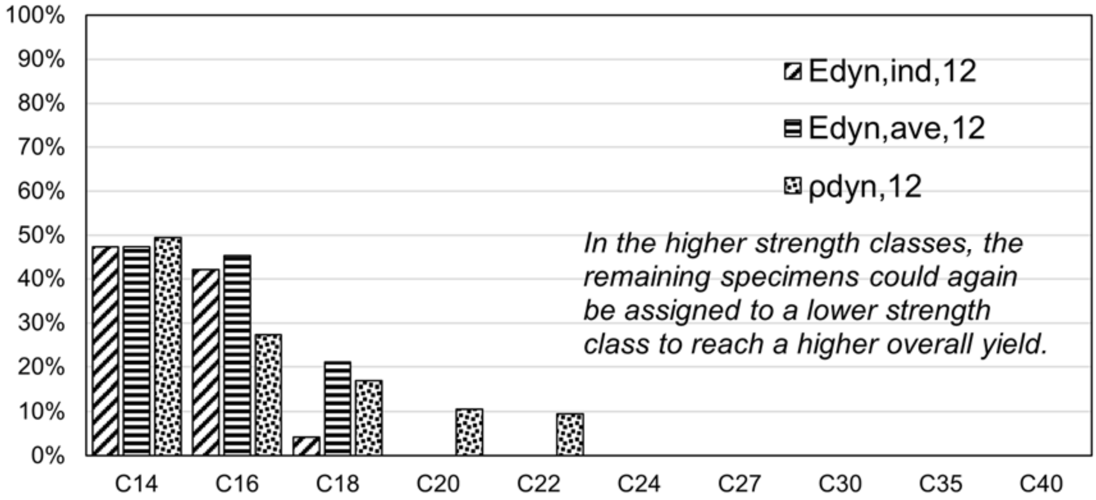

Figure 30: Yield per bending strength class based on the machine grading

4.2.5 Combined Visual and Machine Grading

Considering the previous results, the combined grading approach was investigated using the visual grading parameters DEK and growth ring width and the machine grading parameters dynamic MOE with average density and with individual density as well as the density itself.

By analyzing all possible combinations, the following possible specifications could be identified that allow the assignment of strength classes, see Table 24. The yield of the different strength classes is also presented in Figure 31.

Table 24: Specifications for the combined grading DEK + growth ring width + dynamic MOE with average density and respective characteristic values of the bending test specimens

grading thresholds			characteristic values			yield	assignment to strength class
DEK	growth ring width [mm]	$E_{dyn,ave,12}$ [N/mm²]	$f_{m,k}$ [N/mm²]	$E_{m,0,mean}$ [N/mm²]	ρ_k [kg/m³]		
< 1.0	< 12	> 8000	14.3	8911	354	46 %	C14
< 1.0	< 14	> 9000	16.6	9487	375	36 %	C16
< 1.0	< 14	> 10000	18.6	9844	373	21 %	C18
< 0.4	< 6	> 10000	21.8	11430	399	4 %	C20
< 0.4	< 8	> 10000	25.0	11390	407	5 %	C24

Table 25: Specifications for the combined grading DEK + dynamic MOE with average density and respective characteristic values of the bending test specimens

grading thresholds		characteristic values			yield	assignment to strength class
DEK	$E_{dyn,ave,12}$ [N/mm²]	$f_{m,k}$ [N/mm²]	$E_{m,0,mean}$ [N/mm²]	ρ_k [kg/m³]		
< 0.6	> 9000	15.8	9369	373	29 %	C14
< 1.0	> 9000	16.6	9487	375	36 %	C16
< 1.0	> 10000	18.6	9844	373	21 %	C18
< 0.4	> 10000	25.0	11390	407	5 %	C24

Table 26: Specifications for the combined grading DEK + growth ring width + dynamic MOE with individual density and respective characteristic values of the bending test specimens

grading thresholds			characteristic values			yield	assignment to strength class
DEK	growth ring width [mm]	$E_{dyn,ind,12}$ [N/mm²]	$f_{m,k}$ [N/mm²]	$E_{m,0,mean}$ [N/mm²]	ρ_k [kg/m³]		
< 1.0	< 6	> 8000	14.8	9301	389	33 %	C14
< 1.0	< 14	> 9000	16.3	9473	382	38 %	C16
< 0.4	< 6	> 12000	18.4	11345	416	3 %	C18
< 0.4	< 6	> 11000	20.5	11549	415	5 %	C20

Table 27: Specifications for the combined grading DEK + dynamic MOE with individual density and respective characteristic values of the bending test specimens

grading thresholds		characteristic values			yield	assignment to strength class
DEK	$E_{dyn,ind,12}$ [N/mm²]	$f_{m,k}$ [N/mm²]	$E_{m,0,mean}$ [N/mm²]	ρ_k [kg/m³]		
< 0.5	> 9000	15.1	9451	399	24 %	C14
< 1.0	> 9000	16.3	9473	382	38 %	C16
< 0.4	> 12000	18.4	11345	416	3 %	C18
< 0.4	> 11000	20.5	11549	415	5 %	C20

Table 28: Specifications for the combined grading DEK + growth ring width + density and respective characteristic values of the bending test specimens

grading thresholds			characteristic values			yield	assignment to strength class
DEK	growth ring width [mm]	$\rho_{dyn,12}$ [kg/m³]	$f_{m,k}$ [N/mm²]	$E_{m,0,mean}$ [N/mm²]	ρ_k [kg/m³]		
< 1.0	< 6	> 400	14.8	9301	389	33 %	C14
< 1.0	< 8	> 500	16.3	9698	419	25 %	C16
< 1.0	< 4	> 550	28.0	9008	450	3 %	C18
< 0.8	< 6	> 550	21.9	10245	472	8 %	C20
< 1.0	< 6	> 550	22.4	10340	453	9 %	C22

Table 29: Specifications for the combined grading DEK + dynamic MOE with individual density and respective characteristic values of the bending test specimens

grading thresholds		characteristic values			yield	assignment to strength class
DEK	$\rho_{dyn,12}$ [kg/m³]	$f_{m,k}$ [N/mm²]	$E_{m,0,mean}$ [N/mm²]	ρ_k [kg/m³]		
< 1.0	> 500	15.7	9164	408	29 %	C14
< 0.3	> 500	16.8	10327	328	3 %	C16
< 0.8	> 550	21.9	10245	472	8 %	C20
< 1.0	> 550	22.4	10340	453	9 %	C22

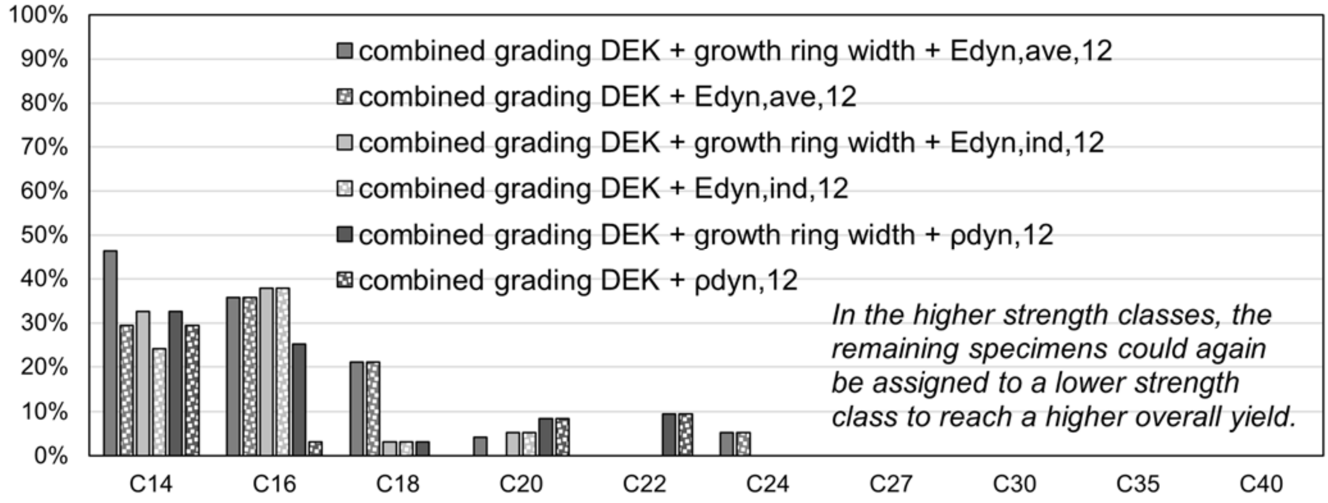

Figure 31: Yield per bending strength class based on the combined visual and machine grading

4.2.6 Comparison of the Different Grading Methods

To compare the different grading methods, Figure 32 and Figure 33 show the yield per strength class of all grading methods. Again, the yield of higher classes was also assigned to lower classes if these had a lower yield, cf. section 4.1.6. Figure 34 shows the highest overall strength class that can be reached by each method.

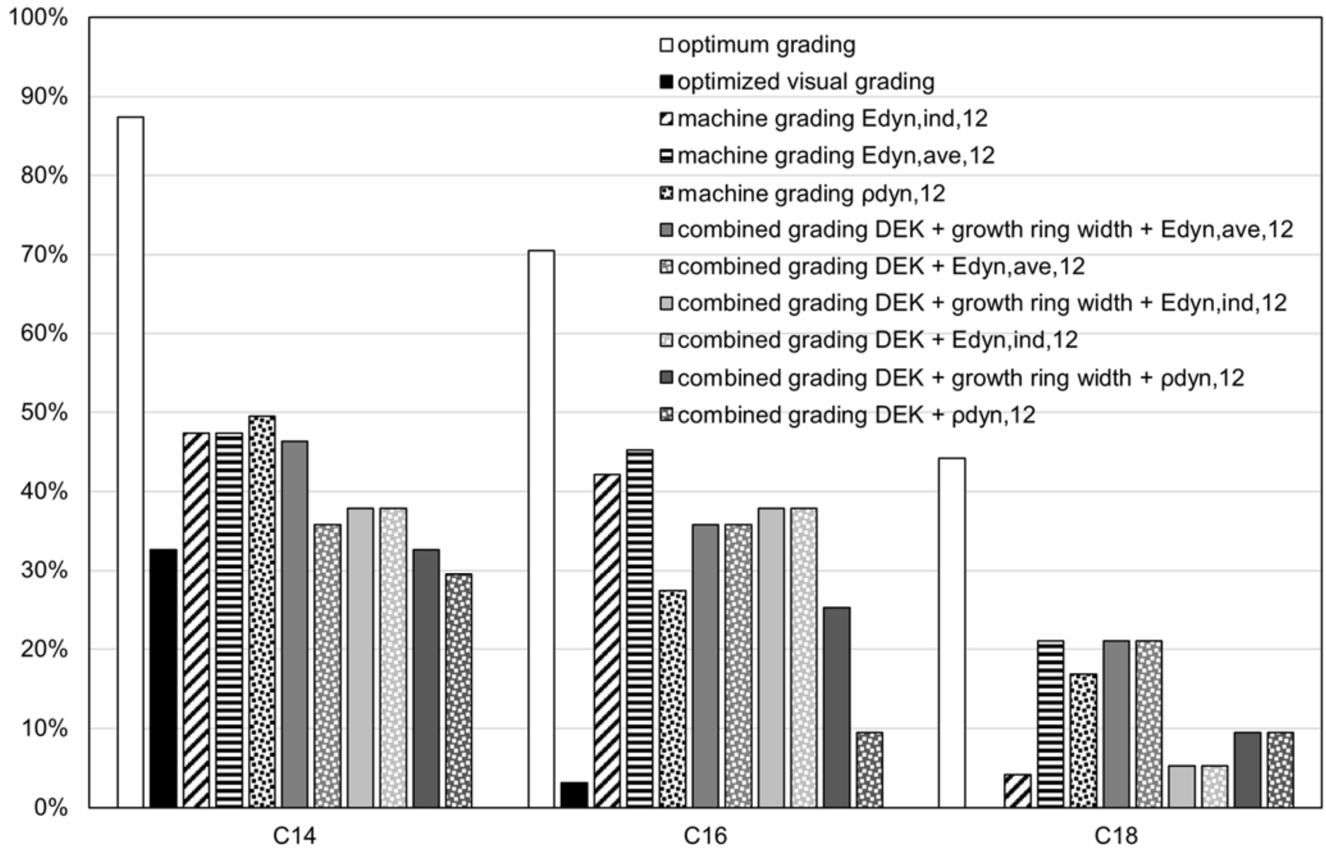

Figure 32: Comparison of the yield of the different grading methods for strength classes C14 to C18

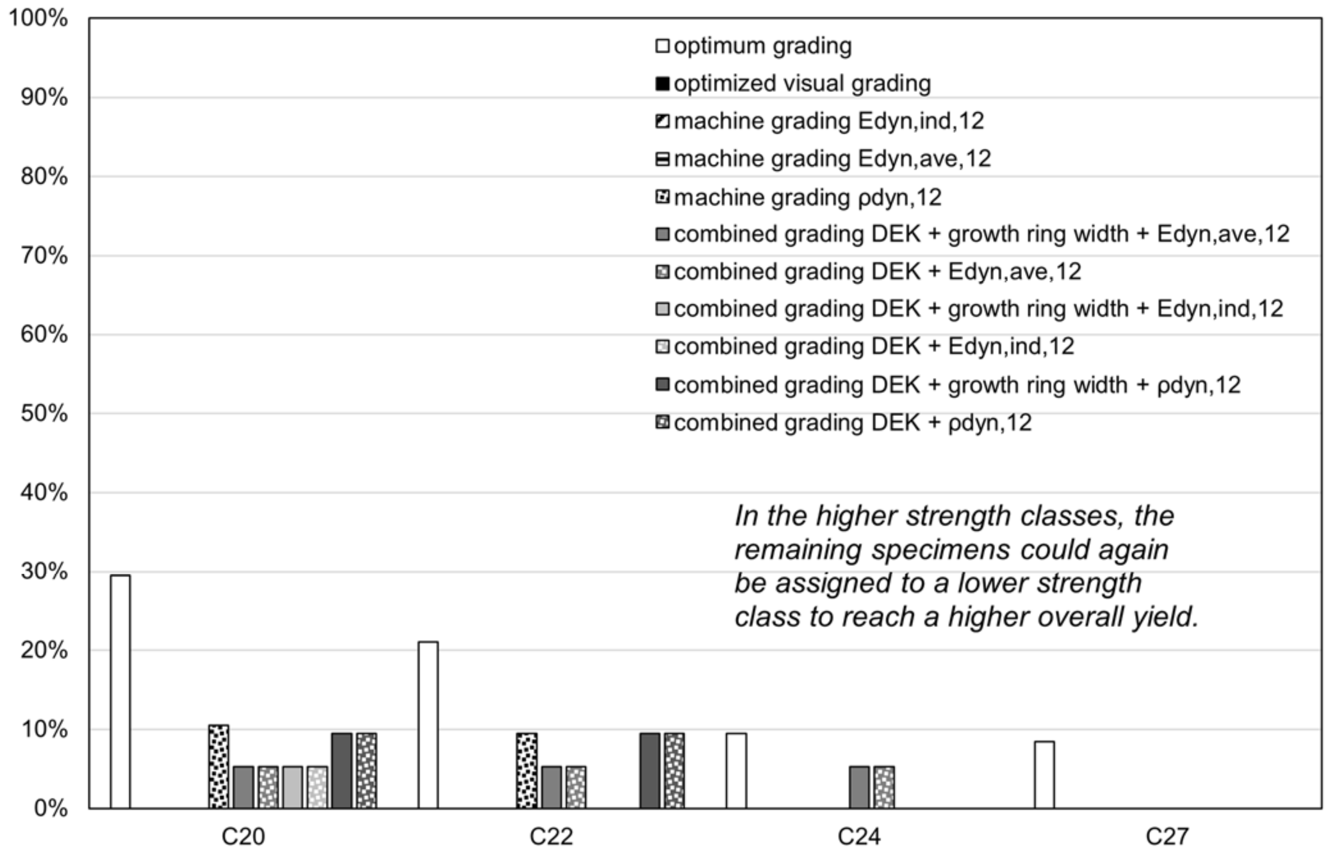

Figure 33: Comparison of the yield of the different grading methods for strength classes C20 to C27

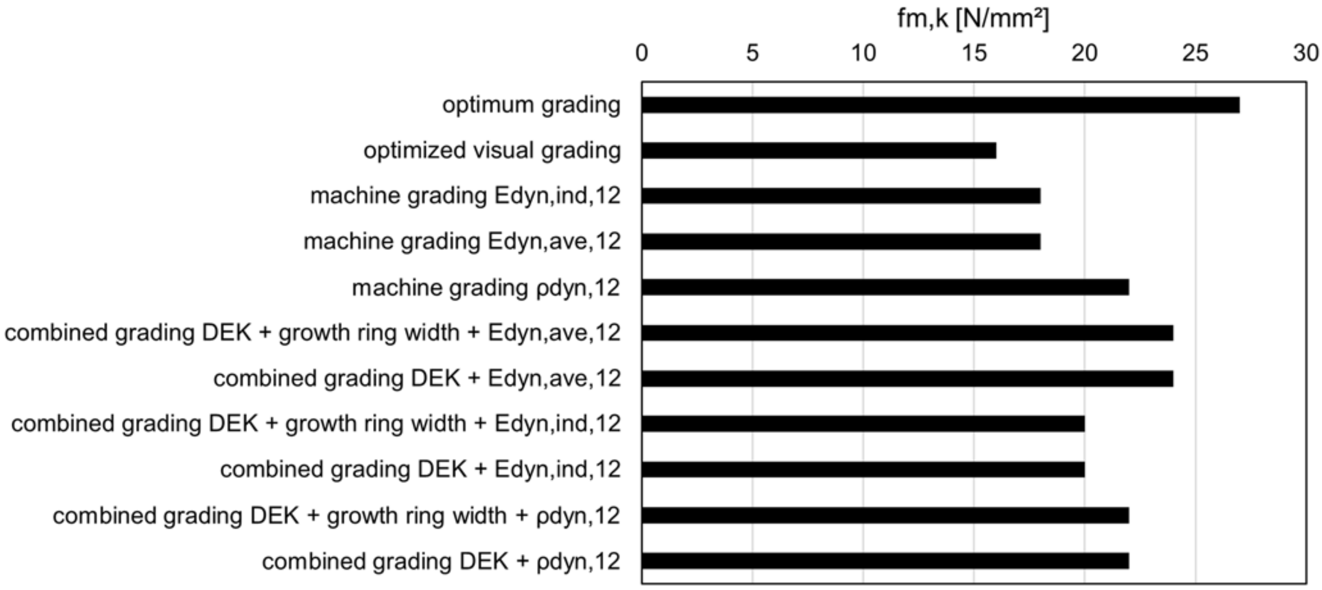

Figure 34: Maximum strength class that the different grading methods can reach

4.3 Bending Tests on Finger Joints

The statistical results according to EN 14358 of the whole sample of bending test specimens with finger joints are shown in Table 30. The relevant values for the assignment of a strength class are highlighted.

Table 30: Statistical values of the bending tests with finger joints according to EN 14358

n = 88	**$f_{m,j}$ [N/mm²]**	**ρ [kg/m³]**
mean	23.5	444
variation coefficient	16.0 %	12.3 %
5th percentile	***17.4***	***349***

Compared to the bending tests without finger joints, the mean values of the strength and the density are similar, but the variation is much lower, so the 5th percentile values are higher. These would fulfill the requirements for the strength class C16 (cf. Table 3) so that finger-jointed structural timber could be produced. For glulam, however, special requirements are defined in EN 14080, see Table 31. These are not met by the investigated sample.

Table 31: Specifications of selected glulam strength classes with required finger joint strengths according to EN 14080

glulam strength class	specifications			
	outer lamellae		inner lamellae	
	strength class	$f_{m,j,k}$ [N/mm²]	strength class	$f_{m,j,k}$ [N/mm²]
GL 20h	T11	22	-	-
GL 24h	T14	30	-	-
GL 24c	T14	31	T9	19
GL 28c	T21	36	T14	26
GL 30c	T22	41	T14	28

h = homogenous, i.e., all lamellae are of the same strength class

c = combined, i.e., lamellae with lower strength class can be integrated into the inner part of the cross-section

Besides the measured strength, the observed fracture modes hint at the quality of the glued connection of the finger joint. Table 32 presents the average percentages of the different fracture modes. The fracture modes are depicted in Figure 35. The outside fracture, meaning a fracture of the wood outside the finger joint with the joint itself staying intact, has the highest percentage. A shear fracture, which indicates a failure of the glue, has the lowest rate.

Table 32: Evaluation of the fracture of the finger joints

	shear fracture	base fracture	outside fracture
average	22.4 %	34.0 %	53.6 %

(a) shear fracture (b) base fracture

Figure 35: Fracture modes of the finger joints tested in bending (Simon Kramer)

4.4 Gluing Tests

The results from the delamination measurement are given in Table 33.

Table 33: Results of the delamination measurement

specimen	delamination	mean delamination
PU 1	7.7 %	10.1 %
PU 2	12.4 %	
MUF 1	3.9 %	3.6 %
MUF 2	3.3 %	

The requirements for the approval of a glue to be used in engineered wood products are given in EN 301 for the MUF glue and in EN 15425 for the PU glue, with a value of 5 % maximum delamination. Thus, the MUF glue would fulfill the delamination requirement, while the PU glue would not. However, for specific products, different requirements may apply.

More tests should be carried out to rule out any errors and inaccuracies. Moreover, additional tests are necessary for the further requirements in the respective standards.

4.5 Fire Tests

The results of the fire tests, including the calculated one-dimensional charring rate, are given in Table 34. The charring rate was calculated at all four measurement points of each specimen.

Table 34: Results of the fire tests

	specimen with higher density	specimen with lower density
ρ_{mean} [kg/m³]	540	405
ρ_k [kg/m³]	450	320
test duration [min]	51:10	46:45
mean charring rate β [mm/min]	0.89	1.01

The density influences the charring behavior. All measurement points at the specimen with higher density gave lower charring rates than those at the lower-density specimen. The mean charring rate is 0.95 mm/min. The charring rate defined in the European standard for fire design is 0.65 mm/min for softwood.

Because of this high deviation, the results from the tests are questionable. The density seems not to be the reason for the deviation; it is 473 kg/m³ on average between the two specimens, which corresponds to European timber of the strength class C35 with a mean density of 470 kg/m³. One possible reason may be the faster charring of the timber at the glued edges, see Figure 36. The thermocouples measuring the temperature within the specimens were arranged inside the joints between the lamellae. The faster charring may be due to higher shrinkage of the individual lamellae, which occurs during the heating and leads to the opening of the joints. The used glue may also be a reason because PU glues are reported to melt during a fire, which facilitates the opening of the joints.

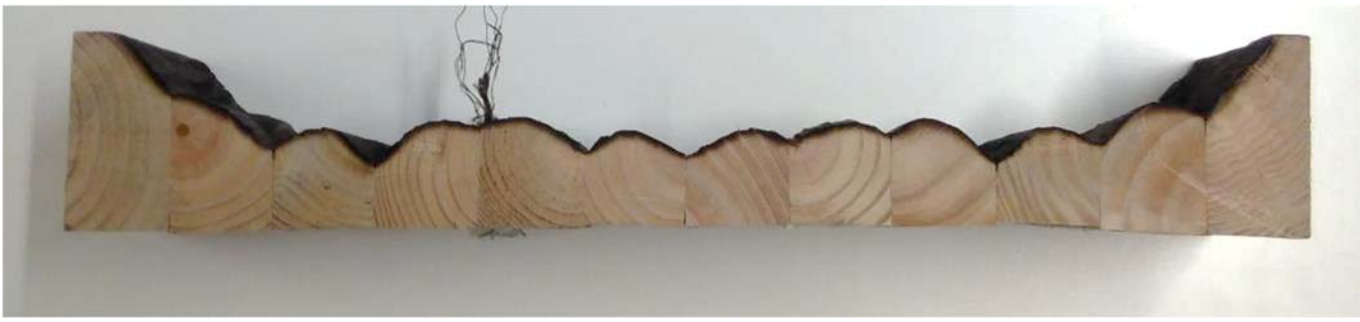

Figure 36: cross-section of a fire test specimen after the test (Lucas Viereck)

To validate the results, further tests are necessary. If material-inherent properties like shrinkage are the reason for the faster charring, this must be considered in a fire design.

4.6 Swelling and Shrinkage

From the measurement of the dimensions and the weight of the specimens at the different climates, multiple parameters concerning the swelling and shrinkage could be calculated, see Table 35.

The maximum linear swelling is the increase in dimension from the oven-dry condition (0 % moisture content) to the saturated condition (> 100 % moisture content) in %. The drying shrinkage is the decrease in dimension from the saturated condition to the standard climate (about 12 % moisture content) in %. Finally, the parameter most used in design of timber structures is the differential swelling, which is the increase in dimension from the dry climate to the moist climate (about 18 % moisture content) in % per % change of the moisture content. The differential swelling is also presented in Figure 37 for the specimens with thin and with wide growth rings separately.

Table 35: Swelling and shrinkage parameters

	specimens with thin growth rings	specimens with wide growth rings	all specimens
maximum linear swelling			
longitudinal	0.3 %	0.5 %	0.4 %
tangential	8.7 %	5.5 %	7.1 %
radial	4.3 %	2.0 %	3.1 %
drying shrinkage			
longitudinal	0.1 %	0.2 %	0.1 %
tangential	4.5 %	2.8 %	3.7 %
radial	2.2 %	0.9 %	1.5 %
differential swelling			
longitudinal	0.01 %/%	0.02 %/%	0.02 %/%
tangential	0.31 %/%	0.19 %/%	0.25 %/%
radial	0.16 %/%	0.29 %/%	0.22 %/%

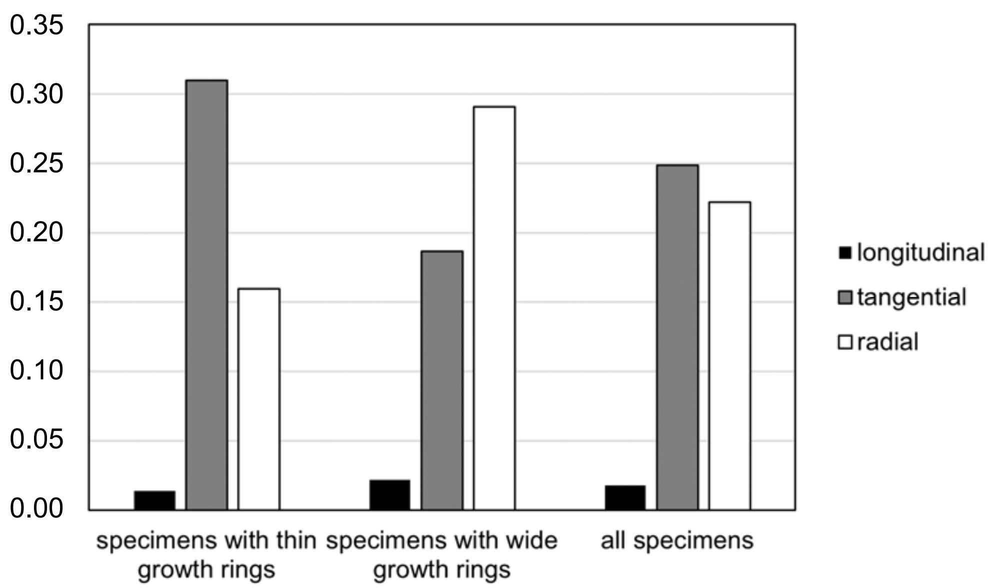

Figure 37: Differential swelling parameters

The swelling in longitudinal direction is negligible ($\alpha = 0.02$ %/%). The swelling in tangential direction is much higher than in radial direction for the specimens with thin growth rings, but much smaller for the specimens with wide growth rings. For practical applications, an average differential swelling of $\alpha = 0.24$ %/% for all growth rings and all directions perpendicular to grain can be used, as is the rule in usual design. European softwood also has a differential swelling of $\alpha = 0.24$ %/%, because it also has thinner growth rings.

5 Summary

Within this research, a sample of pine lamellae from Tanzania has been tested to assess their potential for use in construction. The carried-out tests included a visual grading and a machine grading, tensile tests and edgewise bending tests on individual lamellae, as well as flatwise bending tests on finger joints. These tests lead to statements about the mechanical properties of the Tanzanian timber. Additionally, gluing tests were conducted to assess the suitability of different glues in combination with Tanzanian timber, fire tests were conducted to determine the charring rate of the timber, which is essential for the fire design, and swelling and shrinkage tests were conducted to investigate the behavior of the wood under changing moisture.

The mechanical tests and grading showed that lower strength classes could be reached for Tanzanian-grown pine Pinus patula with sufficient yield. The results of the tensile tests lead to a yield between 47 % and 70 % for the lowest strength class T8, depending on the grading method. The highest tensile strength class that can be reached is T22, with a yield of 7 %, although most grading methods only reached T16. The assignment of the specimens based on the edgewise bending test results led to a yield between 29 % and 49 % for the lowest strength class C14 (comparable to the tensile strength class T8). The highest bending strength class that can be reached is C24, with a yield of 5 % (comparable to T14). However, only C22 (comparable to T13) was possible for most of the applied grading methods.

The direct comparison shows that the tensile tests lead to significantly better results. On the other hand, considering the practical implementation in Tanzania, bending tests usually require less effort.

The recommended grading method leading to the highest yields for the tensile tests and also reaching the highest strength class T22 is a combined grading including the visual grading parameters DEB and DAB (knottiness parameters) and the dynamic MOE from the measurement of the eigenfrequency and the density of each individual specimen. For the specifications of this method, see Table 15. This method has a yield of 63 % in the strength class T8. Alternatively, a different combined grading method can be recommended, which includes the visual grading parameters DEB and DAB as well as the growth ring width and the dynamic MOE from the measurement of the eigenfrequency, but assuming an average density of 460 kg/m³. This method omits the measurement of the density of each lamella, which leads to less technical effort, but it includes the measurement of the growth ring width. Only T16 can be reached with this method, but the yield in these high strength classes is meager anyway (under 10 %). For the specifications of this method, see Table 12. This method has a yield of 67 % in the strength class T8.

For the bending tests, the recommended grading method is the combined grading with the visual grading parameters DEK (knottiness parameter) and the growth ring width together with the dynamic MOE from the measurement of the eigenfrequency, again assuming an average density of 460 kg/m³. With this grading method, the strength class C24 can be reached. For the specifications of this method, see Table 24. This method has a yield of 46 % in the strength class C14.

The bending tests of the finger joints showed that it is possible to finger joint the Tanzanian timber. The characteristic value of the bending strength of the ungraded sample reached 17.4 N/mm², and thus, the requirement for the lowest bending strength class C16 (comparable to T10). However, the requirements for glulam cannot be reached. Still, finger jointing the structural timber may significantly improve the mechanical performance because defects like knots can be cut out.

The gluing tests with two standard types of glue for timber construction proved that it is possible to glue the Tanzanian timber together, an essential requirement for producing engineered wood products. In the carried-out delamination tests, the MUF glue performed a little better, showing 3.6 % delamination on average and thus fulfilling the requirement of 5 % maximum delamination. The PU glue showed 10.1 % delamination. However, the standard delamination test specifications may be questioned because they are very strict and should be adopted to the conditions in Tanzania.

The average charring rate, determined from the fire tests, is 0.95 mm/min, much higher than the assumed charring rate of comparable European timber, which is 0.65 mm/min. The measured value should, therefore, be questioned and validated by further tests.

The swelling and shrinkage proofed to be similar to European softwood, with a differential swelling of $\alpha = 0.24$ %/% perpendicular to grain. However, high warping deformations are possible due to changes in moisture content, that can affect the processibility.

6 Recommendations

The current tests provide only preliminary results and only indicate the possible performance of the Tanzanian-grown pine Pinus patula. The number of specimens for the mechanical tests was not sufficient to satisfy the specifications from EN 384 of at least 40 specimens per grading class or regarding the number of sub-samples. Therefore, the results from this research must be extended by further tests with a more significant number of specimens and sub-samples to cover the variability in the mechanical properties of the Tanzanian pine. Moreover, several samples from different origins should be investigated to avoid a reduction of the characteristic properties (MOE, strength, and density). For only five or more samples, no reduction needs to be made.

Additional tests should be carried out using different types of glues to validate the results of the gluing tests.

Further fire tests are needed to verify the charring rate, preferably using a more heat-resistant adhesive like phenol resorcinol formaldehyde (PRF). The thermocouples should be placed inside the lamellae, not inside the joints.

Literature

Ebert, Nicole (2024): Untersuchung der Eigenschaften von tansanischem Kiefernholz. Bachelor Thesis. Technical University of Munich.

Green Resources (2023): Tanzania Forest Management Plan. Public Summary. Sao Hill, Mafinga. Available online at https://www.greenresources.no/wp-content/uploads/2023/09/GRL_Forest-Management-Plan-2023-Public-Summary.pdf, checked on 6/7/2024.

Hanen, Frederic (2024): Quell- und Schwindmaße von tansanischem Kiefernholz. Seminar thesis. Technical University of Munich.

Henkel & Cie. AG: Loctite HB S109 Purbond. Technical Data Sheet.

Kramer, Simon (2024): Mechanische Kennwerte von tansanischem Kiefernholz. Master Thesis. Technical University of Munich.

Appendix

A. Gluing of the Delamination Specimens

	MUF	PU
amount of glue	400 g/m²	160 g/m²
open waiting time	03:38 min	04:00 min
closed waiting time	07:09 min	06:21 min
pressure	0.8 N/mm²	0.8 N/mm²
press time	21:35 h	21:35 h
storage under standard climate after the pressing	13 days	13 days
time between the cutting of the specimens and the start of the delamination test	5 days	5 days